1-1-2013

Optimization Of Labeling Techniques; Determination Of Best Parameter For Olfactory Mucosal Progenitor Cell Delivery And Study Of Effects Of Methylene Blue And Polyethylene Glycol In An Animal Model Of Spinal Cord Injury

Kiran Kumar Rokkappanavar
Wayne State University,

OPTIMIZATION OF LABELING TECHNIQUES; DETERMINATION OF BEST PARAMETER FOR OLFACTORY MUCOSAL PROGENITOR CELL DELIVERY AND STUDY OF EFFECTS OF METHYLENE BLUE AND POLYETHYLENE GLYCOL IN AN ANIMAL MODEL OF SPINAL CORD INJURY.

by

KIRAN KUMAR ROKKAPPANAVAR

THESIS

Submitted to the Graduate School

of Wayne State University

Detroit, Michigan

in partial fulfillment of the requirements

for the degree of

MASTER OF SCIENCE

2013

MAJOR: BIOCHEMISTRY & MOLECULAR BIOLOGY

Approved by:

_____

Advisor Date

DEDICATION

I dedicate this thesis work to my family for supporting me throughout

and my professor Dr. Jean Peduzzi Nelson who motivated me to do the best I can.

ACKNOWLEDGEMENTS

Many people have played a great part in my graduate education at Wayne State University. I take this opportunity to thank every one of them whole-heartedly.

First and foremost, I owe much credit to Dr. Jean Peduzzi Nelson, my academic advisor who has given me incredible support and devoted time personally to answer all questions and queries I had. She has ably guided me through my work. Interactions with her were always fruitful; supportive and cheerful. I also take this opportunity to convey my regards to Saravanan Kumaran, who taught me all the lab techniques he knew and helped me to design my project. I owe a huge thanks to Dr. George Bittner for collaborating with us. I sincerely thank Dr. Timothy L. Stemmler, Dr. Brian F.P. Edwards and Dr. David R. Evans for being on my thesis committee. I would also like to extend my thanks to Jack Nelson, Jinlan Wang, Sandra Boyce-smith, Rachel Haley, Josh, Scott, Dr. Jonathan King and Norbert Wolf for their help in this project.

I would also like to take this opportunity to extend my thanks to all my friends who have been an integral part of my professional and personal life, especially Poorna, Ashwathy, Gargi, Jyotishko, Yuning. My thanks to all my other friends whom I have got to know over the years for all the company and fun they have given me.

Finally, I would like to thank whole-heartedly, my parents, Mr. Basavaraj R and Mrs. Geetha R, my sister Swetha and my brother Arun for their love and support over the years. It gives me immense pleasure in thanking all near and dear who have stayed by me.

TABLE OF CONTENTS

LIST OF FIGURES

LIST OF TABLES

Chapter 1

Spinal cord injury: Review of literature

1.1 Introduction to Spinal Cord:

There are 31 spinal cord segments, each with a pair of ventral (anterior) and dorsal (posterior) spinal nerve roots, which mediate motor and sensory function, respectively. The ventral and dorsal nerve roots combine on each side to form the spinal nerves that pass through the intervertebral foramina.

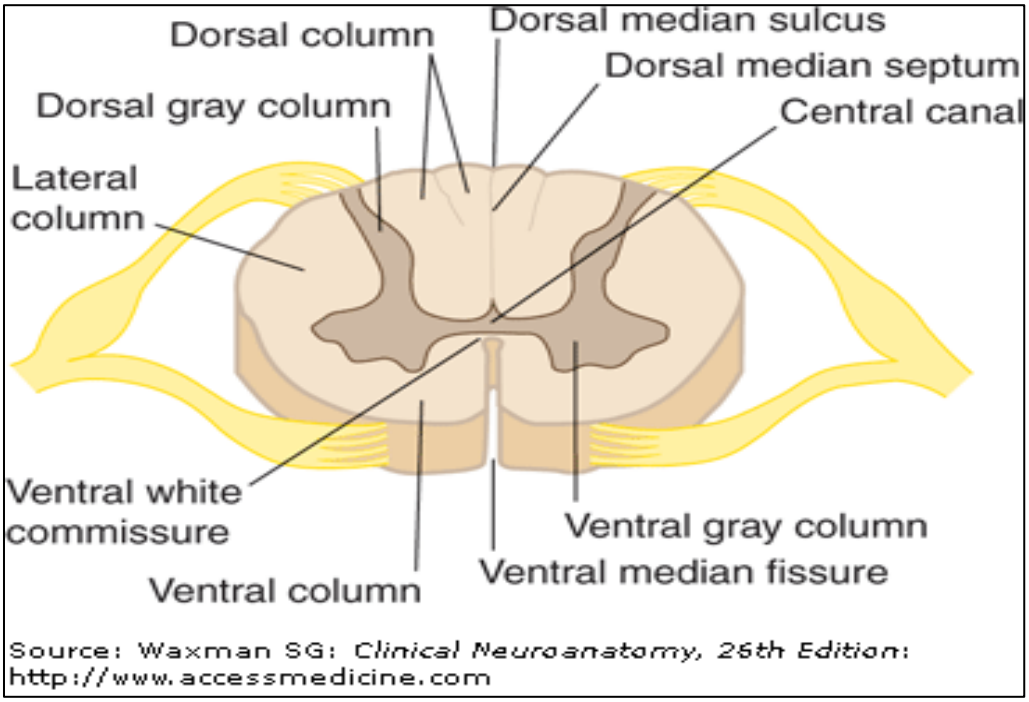

Figure 1.1 Cross section of the spinal cord (*source: Waxman SG: Clinical Neuroanatomy, 26th edition).*

Longitudinal organization — The spinal cord is divided longitudinally into four regions: the cervical, thoracic, lumbar, and sacral cord. The spinal cord extends from the base of the skull

and terminates near the lower margin of the first lumbar vertebral body (L1). Below that level, the spinal canal contains the lumbar, sacral, and coccygeal spinal nerve roots that comprise the cauda equina.

Because the spinal cord is shorter than the vertebral column, vertebral and spinal cord segmental levels are not necessarily the same. The C1 through C8 spinal cord segments lie between the C1 through C7 vertebral levels. The T1 through T12 cord segments lie between T1 through T8. The five lumbar cord segments are situated at the T9 through T11 vertebral levels, and the S1 through S5 segments lie between T12 to L1. The C1 through C7 nerve roots emerge above their respective vertebrae; the C8 nerve root emerges between the C7 and T1 vertebral bodies. The remaining nerve roots emerge below their respective vertebrae.

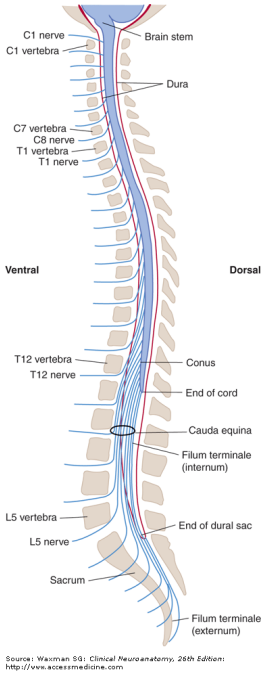

Figure 1.2 Schematic diagram of vertebral column (*source: Waxman SG: Clinical Neuroanatomy, 26th edition)*

Cervical cord — The first cervical vertebra (the atlas) and the second cervical vertebra (the axis), upon which the atlas pivots, support the head at the atlanto-occiput junction. The interface between the first and second vertebra is called the atlanto-axis junction.

- C3 through C5 innervate the diaphragm, the chief muscle of inspiration, via the phrenic nerve
- C4 through C7 innervate the shoulder and arm musculature
- C6 through C8 innervate the forearm extensors and flexors
- C8 through T1 innervate the hand musculature

Thoracic cord — The thoracic vertebral segments are defined by those that have an attached rib. The spinal roots form the intercostal nerves that run along the inferior rib margin and innervate the associated dermatomes, as well as the intercostal abdominal wall musculature. These muscles are the main muscles of expiration. The thoracic cord also contains the preganglionic sympathetic cell bodies that synapse with post-ganglionic neurons that innervate the heart and abdominal organs.

Lumbosacral cord — The lumbosacral spinal cord contains the segments that innervate the muscles and dermatomes of the lower extremity, as well as the buttocks and anal regions. Sacral nerve roots S3 through S5 originate in the narrow terminal part of the cord, called the conus medullaris.

- L2 and L3 mediate hip flexion
- L3 and L4 mediate knee extension
- L4 and L5 mediate ankle dorsiflexion and hip extension
- L5 and S1 mediate knee flexion
- S1 and S2 mediate ankle plantar flexion

Sacral nerve roots also provide parasympathetic innervation of pelvic and abdominal organs, while lumbar nerve roots L1 and L2 contain sympathetic innervation of some pelvic and abdominal organs.

Cauda equina — In adults, the spinal cord ends at the level of the first or second lumbar vertebral bodies. The filum terminale, a thin connective tissue filament that descends from the conus medullaris with the spinal nerve roots, is connected to the third, fourth, and fifth sacral vertebrae; its terminal part is fused to the periosteum at the base of the coccygeal bone.

Pathology at the T12 and L1 vertebral level affects the lumbar cord. Injuries to L2 frequently damage the conus medullaris. Injuries below L2 usually involve the cauda equina and represent injuries to spinal roots rather than to the spinal cord.

Cross-sectional anatomy — The spinal cord contains the gray matter, the butterfly-shaped central region, and the surrounding white matter tracts. The spinal cord gray matter, which contains the neuronal cell bodies, is made up of the dorsal and ventral horns, each divided into several laminae (1,2).

Dorsal horn — The dorsal horn is the entry point of sensory information into the central nervous system. It is divided into six layers or laminae that process sensory information. More than a relay station for the transmission of sensory information, the dorsal horn also modulates pain transmission through spinal and supraspinal regulatory circuits. Three major categories of sensory input that are important to the clinical examination of spinal cord pathology include:

- Afferents from muscle spindles that participate in spinal cord reflexes.
- Axons, mostly small and unmyelinated, mediating sensory modalities of pain and temperature. These can travel up and down a few segments before synapsing with the second order neurons, which then cross the midline of the cord in the anterior

commissure, just anterior to the central canal, and then enter the contralateral anterior or lateral spinothalamic tract.

- Axons mediating the sensory modalities of proprioception, vibration, and touch discrimination. These large myelinated fibers pass through the dorsal horn to enter the ipsilateral dorsal column.

Ventral horn — The motor nuclei of the spinal cord are contained within the ventral horn, which also contains interneurons mediating information from other descending tracts of the pyramidal and extrapyramidal motor systems. These ultimately synapse on the alpha and gamma motor neurons, which subsequently leave the ventral horn via the ventral nerve root to terminate at the neuromuscular junction.

White matter tracts — The major white matter tracts of clinical importance in the assessment of spinal cord disease include:

- The dorsal or posterior columns, the fasciculus gracilis, and the fasciculus cuneatus. These contain sensory information regarding joint position and vibration. They are organized anatomically such that cervical sections lie most laterally and sacral segments most medially. These pathways will cross in the medulla; hence, in the spinal cord, these tracts contain ipsilateral sensory representation.
- The anterior and lateral spinothalamic tracts contain sensory information regarding pain, temperature, and touch. These axons have crossed in the ventral commissure and therefore contain contralateral sensory representation. This tract is somatotopically organized with cervical inputs located most medially and sacral inputs most laterally.
- The corticospinal tracts contain the upper motor neurons that originate in M1 of the primary motor cortex. These axons synapse either directly or indirectly on the anterior horn cells, and as such have distinct sites of anatomic origin within M1 (3). A single

corticomotoneuronal axon synapses with many anterior horn cells of its own motor neuron pool and also with those of agonists and antagonists, allowing for coordination of highly skilled movements.

The lateral corticospinal tract contains the majority (80 to 85 percent) of these fibers, which have previously decussated (crossed) at the cervicomedullary junction and therefore provide input to the ipsilateral musculature. Fibers are somatotopically organized within the tract such that fibers destined for upper extremity motor control lie most medially, while fibers controlling the lower extremity lie more laterally. The anterior corticospinal tract contains undecussated fibers, some of which will subsequently cross at the spinal level through the anterior commissure.

Autonomic fibers — Autonomic fibers of hypothalamic and brainstem origin descend in the lateral aspect of the spinal cord. These synapse with cell bodies in the intermediolateral columns of the central gray matter of the spinal cord. Sympathetic fibers exit between T1 and L2, and parasympathetic fibers exit between S2 and S4.

Autonomic dysfunction is an important determinant of site, extent, and severity of spinal cord pathology. Many autonomic functions can be affected by spinal cord pathology, but for clinical evaluation, the most useful symptoms relate to bladder control.

Autonomic bladder control is primarily parasympathetic, and is unaffected by isolated injury to the sympathetic fibers. Voluntary bladder control is under somatomotor control, mediated by motor fibers originating from the anterior horn cells at levels S2-S4. A spinal cord lesion that interrupts descending motor and autonomic tracts above the S2 level produces an "automatic bladder" that cannot be emptied voluntarily, but empties reflexly when expanded to a certain degree, the so-called neurogenic bladder (4, 5, 6). Loss of descending inhibition of segmental reflex control leads to urinary urgency and incontinence. Injury to S2-S4 spinal levels

interrupts the bladder reflex circuit; the bladder becomes flaccid, and fills beyond capacity with overflow incontinence.

Blood supply — A single anterior and two posterior spinal arteries supply the spinal cord. The anterior spinal artery supplies the anterior two-thirds of the cord (7, 8, 9, 10, 11). The posterior spinal arteries primarily supply the dorsal columns. The anterior and posterior spinal arteries arise from the vertebral arteries in the neck and descend from the base of the skull. Various radicular arteries branch off the thoracic and abdominal aorta to provide additional blood supply to the spinal arteries.

1.2 Anatomical and Functional Changes after Injury

The types of disability associated with spinal cord injury vary greatly depending on the severity of the injury, the segment of the spinal cord at which the injury occurs, and which nerve fibers are damaged. In spinal cord injury, the destruction of nerve fibers that carry motor signals from the brain to the torso and limbs leads to muscle paralysis. Destruction of sensory nerve fibers can lead to loss of sensations such as touch, pressure, and temperature; it sometimes also causes pain. Other serious consequences can include exaggerated reflexes; loss of bladder and bowel control; sexual dysfunction; lost or decreased breathing capacity; impaired cough reflexes; and spasticity (abnormally strong muscle contractions). Most people with spinal cord injury regain some functions between a week and six months after injury, but the likelihood of spontaneous recovery diminishes after six months. Rehabilitation strategies can minimize the long-term disability.

Spinal cord injuries can lead to many secondary complications, including pressure sores, increased susceptibility to respiratory diseases, and autonomic dysreflexia. Autonomic dysreflexia is a potentially life-threatening increase in blood pressure, sweating, and other

autonomic reflexes in reaction to bowel impaction or some other stimulus. Careful medical management and skilled supportive care is necessary to prevent these complications.

Researchers studying spinal cords obtained from autopsy have identified several different types of spinal cord injuries. The most common types of spinal cord injuries found in one large study were contusions (bruising of the spinal cord) and compression injuries (caused by pressure on the spinal cord) (12). Other types of injury included lacerations, caused by a bullet or other object, and central cord syndrome.

In contusion injuries, a cavity filled with CSF often forms in the center of the spinal cord due to the death of cells in that regions. Myelinated axons typically survive in a ring along the inside edge of the cord. Some axons may survive in the center cavity, but they usually lose their myelin covering. This demyelination greatly slows the speed of nerve transmission. Slowing of nerve impulses can be measured by a diagnostic technique called transcranial magnetic stimulation (TMS).

Another example of a spinal cord injury is central cord syndrome, which affects the cervical (neck) region of the cord and results from focused damage to a group of nerve fibers called the corticospinal tract. The corticospinal tract controls movement by carrying signals between the brain and the spinal cord. Patients with central cord syndrome typically have relatively mild impairment, and they often spontaneously recover many of their abilities. Patients usually recover substantially by 6 weeks after injury, despite continued loss of axons and myelin. Delays in motor responses persist, but permanent impairment is usually confined to the hands. (12)

1.3 Epidemiology

Most demographic and epidemiological data related to traumatic spinal cord injury (TSCI) in the United States have been collected by the Model Spinal Cord Care Systems and

are published by the National Spinal Cord Injury Statistical Center (13). In the United States, the incidence of TSCI is about 40 per million persons per year, with approximately 250,000 living survivors of TSCI in the United States in July 2005.

The causes of TSCI in the United States are (14):

- Motor vehicle accidents: 47 percent
- Falls: 23 percent
- Violence (especially gunshot wounds): 14 percent
- Sports accidents: 9 percent
- Other: 7 percent

Statistics differ somewhat in other countries. In Canada and western Europe, TSCI due to violence is rare, while in developing countries, violence is even more common (15, 16)

Risk factors for TSCI have been identified. Prior to 2000, the most frequent victim was a young male with a median age of 22. Since that time, the average age has increased in the United States to 38 years, presumably as a reflection of the aging population. Males continue to make up 80 percent of cases (15, 16, 17). Alcohol plays a role in at least 25 percent of TSCI (18, 19). Underlying spinal disease can make some patients more susceptible to TSCI (18, 20). These conditions include:

- Cervical spondylosis
- Atlantoaxial instability
- Congenital conditions, e.g., tethered cord
- Osteoporosis
- Spinal arthropathies, including ankylosing spondylitis or rheumatoid arthritis

1.4 Classification of SCI:

The mechanisms surrounding injury to the spinal cord itself are often discussed in terms of primary and secondary injury. The primary injury refers to the immediate effect of trauma which includes forces of compression, contusion, and shear injury to the spinal cord. In the absence of cord transection or obvious hemorrhage (both relatively rare in nonpenetrating injuries), the spinal cord may appear pathologically normal immediately after trauma. Penetrating injuries (e.g. knife and gunshot injuries) usually produce a complete or partial transection of the spinal cord. An increasingly described phenomenon, however, is a spinal cord injury following a gunshot wound that does not enter the spinal canal (21). Presumably, the spinal cord injury in these cases results from kinetic energy emitted by the bullet.

A secondary, progressive mechanism of cord injury usually follows, beginning within minutes and evolving over several hours after injury (18, 22, 23). The processes propagating this phenomenon are complex and incompletely understood. Possible mechanisms include ischemia, hypoxia, inflammation, edema, excitotoxicity, disturbances of ion homeostasis, and apoptosis (18). The phenomenon of secondary injury is sometimes clinically manifest by neurologic deterioration over the first 8 to 12 hours in patients who initially present with an incomplete cord syndrome.

As a result of these secondary processes, spinal cord edema develops within hours of injury, becomes maximal between the third and sixth day after injury, and begins to recede after the ninth day. This is gradually replaced by a central hemorrhagic necrosis.

1.5. Axonal Damage following SCI

With the current scientific excitement about cell death, it is important to emphasize that damage to axons causes most of the problems associated with spinal cord injury, including loss of motor control and sensation. In rat spinal cord contusion injuries, for example, recovery of

function correlates closely to the number of remaining axons. Until recently, most researchers assumed that the physical forces of spinal cord trauma immediately tear axons. Recent studies of axon damage following traumatic brain injury are changing this view.

Within several days of traumatic brain or spinal cord injury, grossly swollen axons, termed "reactive swellings" or "retraction balls," appear (12). Many scientists believe that physical forces of trauma stretch axon fibers, causing them to tear and swell. Studies using multiple animal models and various anatomical tracers now have shown that much of the axon damage following CNS trauma is not immediate. Instead, it occurs hours later from swelling caused by impaired axonal transport. Axonal transport is a vital cellular process that moves molecules and cell components from the cell body toward the axon terminal and from the terminal back to the cell body.

What disrupts axonal transport and causes delayed axon damage? There appear to be multiple causes, but changes to the cytoskeleton play a critical role (24). The cytoskeleton is the internal scaffolding that determines the shapes of cells. It is necessary for transport of substances along the axons. In severe injuries, changes in the cell membrane that surrounds axons can allow an abnormal influx of ions, particularly calcium. This leads to compacting of the cytoskeleton and interruption of axonal transport. Calpain, a calcium-activated protein-degrading enzyme, probably participates in this process. Swelling and disrupted transport also occur in axons whose membranes show no change in ion permeability. In these axons, which predominate in mild to moderate injuries, neurofilaments (one component of the cytoskeleton) become misaligned. This, again, impairs transport and leads to swelling of axons.

Damage to axons has several consequences within the spinal cord. Following axon injury, axons disconnected from their nerve cell bodies disintegrate by a process called "Wallerian" or "orthograde" degeneration.

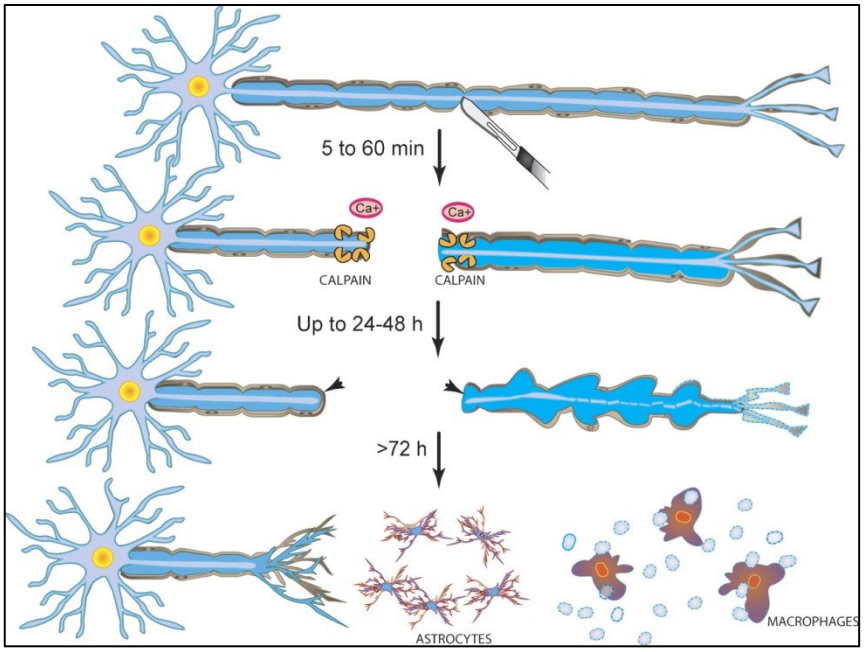

Figure 1.3 Schematic diagram showing the changes seen in Wallerian degeneration *(source: Wang J T et al. J Cell Biol 2012;196:7-18).*

Nerve cell bodies with damaged axons, and the axon segment that remains attached, may die by retrograde degeneration, that is, degeneration that begins at the site of injury and progresses back toward the cell body. From a functional point of view, the delayed death of oligodendrocytes and the resulting demyelination of axons are also critical events, because unmyelinated axons do not conduct electrical impulses normally. The death of these glial cells may result partly from the degeneration of damaged axons because oligodendrocytes apparently require contact with axons to remain healthy. The removal of normal nerve connections also has important consequences. The diverse effects of axon injury suggest that more than one therapeutic approach may be needed to overcome this damage.

1.6 Review on Treatment of SCI:

Various methods have been tried to restore the functionality of the nervous system following SCI. One approach is high doses of anti-inflammatory steroids. However, the greatest

effects of steroids on spinal cord injury may relate to their antioxidant action, specifically its ability to combat lipid peroxidation. Steroids may be neuroprotective in preventing secondary injury and have been tried in many of the preclinical trials as a therapy for SCI. Methylprednisolone was extensively studied in 5 prospective human trials (25).The National Acute Spinal Cord Injury Study (NASCIS) trials used MethylPrednisolone Sodium Succinate (MPSS) but some patients developed serious adverse events such as pulmonary embolism, pneumonia, sepsis and death (26).

Another approach to treat spinal cord injury is to block the inhibitors of axonal growth. Many of the endogenous chemicals (Nogo, Myelin Associated Glycoprotein and Oligodendrocyte Myelin Glycoprotein) accumulate in the environment of the axons following SCI which hamper neuronal regeneration (27). Accordingly, various agents have been tried to block such inhibitors. Anti-Nogo-A antibodies were designed to block Nogo molecules but they did not achieve success (28, 29). Botulinum toxin C3 specifically inactivates Rho factor by ADP ribosylation of its active site thereby inhibiting growth cone collapse that occurs in response to myelin and MAG (30). Boato and colleagues observed that there was significant improvement in injuries involving corticospinal tract when enzyme deficient Clostridium botulinum C3-protein-derived 29-amino-acid fragment c3bot was used (31). 'Semaphorin 3A' is another molecule which interferes with axonal regeneration. A selective inhibitor of semaphorin 3A, SM-216289 derived from a fungus was injected at the injury site. There was a significant improvement in axonal regeneration (32).

The glial scar is believed to inhibit recovery so efforts have been made to disrupt the scar. Following an injury in the CNS, a glial scar develops at the site that contains extracellular matrix molecules such as chondroitin sulfate proteoglycans (CSPGs) (33, 34). They have a negative effect on neuronal regeneration as a physical and/or chemical blocker of regeneration. Chondroitinase ABC, an enzyme that can break the complex molecular structure of CSPG,

when given intrathecally promoted the growth of sensory and motor neurons (35). Other groups have given mixed results for similar studies.

Another approach to spinal cord injury is cell transplantation. Olfactory ensheathing cells (OECs) are glial cells of the olfactory system that produced functional improvement when transplanted into the injury site in a model of spinal cord transections (36). These cells may encourage the growth of axons or they may myelinate. Animal models of spinal cord injury often use progenitor stem cells derived from bone marrow. These cells have given both positive (37) and negative results (38). The cells can be easily obtained with a bone biopsy so autologous cells could potentially be used in future clinical studies. Another cell type that might have potential for autologous transplant in future clinical studies is olfactory mucosa progenitor cells (39). Human embryonic stem cells effectively promoted motor function in mice (40) and rats (41). These cells also promoted corticospinal tract regeneration in rats (42). These cells are associated with ethical concerns and may be rejected or form tumors. Oligodendrocytes differentiated from embryonic stem cells were used in a clinical trial by Geron for subacute spinal cord injury. The trial was stopped after investment of 250 million dollars (43). On the other hand, induced pluripotent stem cells (iPSCs) are gaining popularity in preclinical studies because these cells derived from an adult cell would avoid the problem of rejection found with embryonic stem cells if used clinically (44)

1.7 Stem cells

Stem cells are known for their remarkable potentiality to differentiate into many different cell types in the body throughout the life of the organism (45). Under the right conditions or given the appropriate signals, stem cells can become different cell types through asymmetric cell division. Each new cell formed by the division of stem cells has the potential to remain as a stem cell or to become another type of specialized cell with a different function. Stem cells also function as an internal repair system, dividing essentially to repair and replace damaged tissues.

Biologic therapies derived from such cells are expected to be effective in treatment of a wide range of medical conditions, which is also referred to as regenerative or reparative medicine.

In neurological diseases, the aim of cell therapy is to replace, repair, or enhance the biological function of damaged cells in order to restore or receive brain functions (46). This may occur through delivery of trophic factors and neurotransmitters, buffering toxic molecules and providing favorable cell–cell communication. A variety of stem cells were shown to differentiate into major neural cells in brain tissue (neurons, astrocytes, and oligodendrocytes) (47). Three major groups of cells with neurogenic potential have been identified: neural progenitor cells derived from embryonic or adult nervous tissue (48, 49), nonneural progenitor cells derived from other tissues and organs (50, 51) and embryonic stem cells from the early embryo (52, 53).

1.8 Olfactory mucosal stem cells

Olfactory mucosa progenitor cells are obtained from tissue located in nasal passageways (uppermost part of the inside of the nose). There are several advantages of these cells beyond the fact that these cells can also be obtained with minimally invasive techniques (54). In contrast to other readily available sources of adult stem cells, the normal fate of olfactory mucosa progenitor cells is to become neurons and neural support cells (55, 56). Olfactory mucosa neural progenitor cells maintain telomerase activity and low apoptotic activity after several years in culture. Unlike hematopoietic stem cells and bone marrow mesenchymal cells, the capacity to replicate does not change with a person's age (57). In addition, the olfactory mucosa is the only portion of the adult nervous system capable of lifelong neurogenesis (58, 59, 60, 61, 62, 63, 64). Clinical and basic science studies provide evidence that when stem cells are injected into the cerebrospinal fluid, the stem cells home to the injured area, penetrate the brain and induce recovery (65, 66). If this treatment proves to be effective and moves to clinical trials, a person's own stem cells could be used for the treatment avoiding the problems of rejection or disease transmission in traumatic brain injury.

Chapter 2

Progenitor cells and Spinal Cord Damage / Comparison of different routes of stem cell transplantation

2.1 Models of SCI

Even though there are various types of SCI models, majority of them can be classified into 5 categories based on the morphologic, histologic and imaging characteristics: Solid cord injury, Laceration, Maceration / Compression, Contusion & Chemical induced. (67)

Solid cord injury: Those injuries that could be classified into this category account for nearly 10 % of all clinical cases. These are basically injuries involving white matter. Even though on gross appearance spinal cord appears normal, but on histological analysis one can visualize dorsal column demyelination and loss of motor neurons. The best example for this type of lesion is Multiple Sclerosis.

Laceration: This type of injury usually results when a sharp object such as an object or a fragment of bone penetrates the spinal cord. In this type of injuries, meninges are disrupted resulting in systemic cell infiltration and scar formation at the epicenter of the lesion, which is often seen as adhering to the overlying dura. Animal models for this type of injury include hemi- or bilateral transection of the cord in which spinal cord would be exposed, tissue severed with a sterile sharp object. Also, suction may be applied to selectively destroy motor or sensory tracts. The major advantage of this model is its complete control over the location and the size of the lesion. Also this model enables the researcher to effectively quantify the regeneration techniques following the injury. The disadvantage with this type of injury is the limited number of clinical cases (only 21%).

Maceration or Compression: This type of injury results when a massive compression force is applied to the spinal cord. Generally the force is applied more slowly than a contusive type injury. When this happens, the anatomy of the spinal cord is disrupted and a very few fibers could be seen running the long axis of the spinal cord. This type of injury can be induced in animals by any of the methods listed: aneurysm clips, epidural balloons, subdural balloons. This produces an ischemic injury. These techniques basically disrupt the blood flow to spinal tissue resulting in injury that simulates maceration or compression. The disadvantage with these types of injury models are that only 20 % of clinical cases fall into this type of injury category. *Contusion*: This is the largest category of spinal cord injury, it is caused by a focal hemorrhage or necrosis that eventually results in a fluid filled cyst at the epicenter with a rim of normal tissue at the pial surface of the cord. The secondary injury makes the lesion much larger than the original injury. Later there is apoptotic cell death, which destroys additional cells. As the meninges remain intact in contusions, the systemic cell infiltration is less. On histological analysis, there is little connective tissue after a contusive injury because the meninges are intact that prevent the invasion of the fibroblasts. The great advantage of this injury model is that it addresses the maximum number of clinically observed cases (50%). This type of injury can be induced by several methods: the MASCIS (Multicenter Animal Spinal Cord Injury Study) device, the OSU (Ohio State University) device called the IH (Infinite Horizon) device, or any other modified weight drop devices. These methods induce injuries that can be pathophysiologically comparable to human cases of SCI. Another advantage of this injury model is that the injury can be induced at different levels of severity depending on the amount of weight used to drop. Contusions created using 200-230 kilo dynes induce mild spinal cord injury; Contusions ranging 250-290 kilo dynes induce moderate spinal cord injury; and a force of >300 kilo dynes induces severe spinal cord injury. (68).

Chemically induced SCI: Various chemicals have been used to achieve targeted neuronal death. Intrathecal delivery of kainate results in death of both oligodendrocytes and

neurons. (69, 70). Kainate or TNF-alpha when injected into the spinal cord cause degeneration of gray matter. Free radicals also cause spinal cord injury by destroying the axonal conduction system. Examples include herbicide paraquat, a powerful superoxide generator, hydrogen peroxide and FeCl2, S- or 3- morpholinosydnonimine donors, and peroxynitrite donors (71, 72). When zomosan, a yeast derivative is injected, it activates microglia/macrophages that induce inflammation in both white and gray matter creating a similar pathology that is seen following traumatic SCI (73). Phospholipase A2 is a family of enzymes that can generate precursors of inflammatory mediators involved in spinal cord inflammatory disease (73). Other chemicals used for this purpose are ethidium bromide (74), cholera toxin B-subunit conjugated to saporin (75), kaoline suspension (76), and quisqualic acid (77).

2.2 The MASCIS impactor

The MASCIS Impactor is a device designed to deliver graded reproducible spinal cord contusions in rats. It is a part of a well-defined rodent spinal cord injury model that is used in many laboratories around the world. Most of the recommended procedures for the Impactor are based on experience with the model and work done by the Multicenter Animal Spinal Cord Injury Study (MASCIS) (Figure 2.1). The Impactor is now in its third generation with many improvements over previous models.

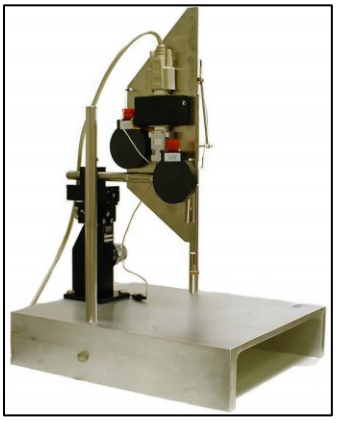

Figure 2.1 Multicenter Animal Spinal Cord Injury Study (MASCIS) impactor *(source: W.M.Keck Center for Collaborative Neurosciences)*

The MASCIS Impactor, formerly called the NYU Impactor, was developed in 1991 by Drs. John Gruner, Carl Mason, and Wise Young and is now widely used in studies of spinal cord injury. The device precisely measures the movement of a 10-gram rod dropped 12.5, 25.0, or 50.0 mm onto the T9-10 spinal cord exposed by laminectomy. The device has greatly reduced the risk of multiple injuries because of drop weight "bounce." In addition, the device measures movement of the spinal column at the impact site, displays the trajectory of the falling rod, and measures the impact velocity (ImpV), cord compression distance (Cd), cord compression time (Ct), and cord compression rate (Cr). These impact parameters correlate with each other and spinal cord lesion volumes (estimated from tissue Na^+ and K^+ concentrations) and locomotor recovery (BBB scores. Basso DM, 1995). Following most SCI in humans, the bone impacts the spinal cord causing contusion. Whereas in the MASCIS model, the rod is dropped from a certain height (representing impact by bone) onto the dural surface after removing the lamina of the vertebral column. This differs from human SCI in that there is room for swelling. Specific training protocols have been developed for the MASCIS Impactor. These are taught in the Keck Center International Spinal Cord Injury Workshop, which is offered four times a year.

2.3 CTB-SAP

Specific motor neurons can be destroyed by injecting muscles with cholera toxin B-saporin (CTB-SAP). This conjugate binds to the GM1 ganglioside receptor found on motor neurons; the complex is then internalized. Saporin (SAP, ribosome inactivating protein) is retrogradely transported from the neuromuscular synapse back to the cell body in the spinal cord where it inactivates the ribosomes,

Figure 2.2 Effect of CTB-SAP: Left: CTB^+ cells in spinal cord. Right: Lack of CTB^+ cells after CTB-SAP injection.

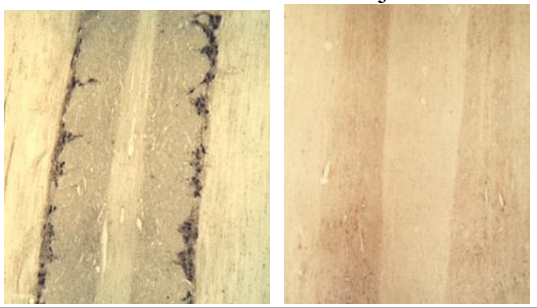

inhibiting protein synthesis and ultimately causing neuronal death. Motor neurons at particular levels of the spinal cord can be selected because the spinal level of innervation of muscles is known (79). Our lab has previously used this method to selectively kill neurons in the spinal cord (Figure 2.2) (80, 81). Others have also used this technique to selectively destroy certain motor neurons in the brain (82) and lumbar spinal cord (83, 84, 85) but never as a way of evaluating a progenitor cell treatment. One advantage of using CTB-SAP is that motor neurons on one side can be destroyed with the complex while those on the opposite side receive only the non-toxic CTB and thereby serves as a convenient control.

2.4 Types of Stem cells:

1. Embryonic stem cells: These pluripotent stem cells are derived from the inner cell mass of the blastocyst (a stage when embryo consists of 50-150 cells) (86) or from germinal cells or from germ cells from 5-9 week old embryos (87). Even though they have ability to differentiate into any type of cell in the body, it has not been possible to treat human diseases with them because they are frequently rejected by the immune system and form tumors. ESCs attacked by the host immune cells are completely eliminated from the body within a matter of days. Even with the use of immunosuppressive agents like tacrolimus, sirolimus and mycophenolate mofetil, ESCs barely survive past 3-4 weeks following transplantation (88, 89). Also ethical issues also limit their use in clinical medicine.

2. Adult Stem Cells: Also known as Somatic Stem Cells (SC), these are undifferentiated cells found throughout the body, most of the time located near the tissues where they serve to replenish the dying cells and regenerate damaged tissues. Unlike ESCs, there are no controversies involved in their usage as they are derived from adult tissue samples rather than destroyed human embryos. Examples include: Hematopoietic SC, Mammary SC, Intestinal SC, Mesenchymal SC, Endothelial SC, Neural SC, Olfactory adult SC, Neural Crest SC, and Testicular SC (90). Unlike hematopoietic stem cells and bone marrow mesenchymal cells, the

capacity to replicate does not change with a person's age (57). The olfactory mucosa is the only portion of the adult nervous system capable of lifelong neurogenesis (58, 59, 60, 61, 62, 63, 64). In contrast to embryonic or fetal derived neural stem cells, which form tumors, Olfactory Mucosa Progenitor Cells (OMPCs) are free of such unregulated growth. The ease of isolating and maintaining these cells has made them widely used. They can be obtained from all individuals, including the elderly, from whom they are needed the most. Another advantage of using OMPCs is that the cells can be transplanted intrathecally using a routine medical procedure to reach the site of lesion. Clinical and basic science studies provide evidence that when stem cells are injected into the cerebrospinal fluid, the stem cells home to the injured area, penetrate the brain and induce recovery (65, 66). If this treatment proves to be effective and moves to clinical trials, a person's own stem cells could be used for the treatment avoiding the problems of rejection or disease transmission in traumatic brain injury.

3. Induced Pluripotent Stem Cells: These are a type of pluripotent stem cells derived from non-pluripotent stem cells by forcefully inducing them to express certain genes. As with ESCs, these are also have a propensity to form tumors (91) seriously limiting their use. These cells when injected into the immunodeficient mice, formed teratoma, questioning their safety because FDA considers teratoma formation as a major obstacle for the stem-cell based therapies in regenerative medicine. Key transcription factors could be used on hepatocytes and gastric epithelial cells to create germline chimeras in mice. Such iPSCs look similar to stem cells in terms of gene expression and ability to create germline chimeras (92).

2.5 Methods of labeling stem cells:

After the stem cells are transplanted, it is important to test their survival, integration into the host tissue and phenotype in terms of whether or not the cells have differentiated. For this purpose, stem cells are labeled using several different methods. Stem cells can be labeled with lipophilic fluorescent dye DiD (C67H003CIN203S) which crosses the phospholipid cell

membrane and concentrates in the cytoplasm. Stem cells (hESC) can also be labeled with Indocyanine Green (ICG), which is lipophilic. Its efficacy can be improved with the addition of serum-free media and the usage of a transfection agent. Furthermore, addition of protamine sulfate significantly improves the uptake of the dye. (93). Bromodeoxyuridine (5-bromo-2-deoxyuridine, BrdU) is a synthetic nucleoside that can be incorporated into the newly synthesized DNA of replicating cells. The BrdU-containing cells can be subsequently detected by immunochemistry using a BrdU-specific antibody (94, 95).

One type of fluorescent dye used to label cells only fluoresces when it enters the cells. Carboxy Fluorescein DiAcetate Succinimidyl Ester (CFDA-SE) is a fluorescent cell staining dye Figure 2.3). CFDA-SE, due to its acetate groups, is highly cell permeable. CFDA-SE is colorless and non-fluorescent, but when it enters the cytoplasm of cells, intracellular esterases remove the acetate groups of CFDA and convert the molecule to the fluorescent ester, CFSE, which is retained within cells and covalently coupled, via its succinimidyl group, to intracellular molecules (96). Due to this covalent coupling reaction fluorescent CFSE can be retained within cells for extremely long periods. Also, due to this stable linkage, once incorporated within cells the dye is not transferred to adjacent cells. CFSE was originally developed as a fluorescent dye that could be used to stably label lymphocytes and track their migration within animals for many months (97). Subsequent studies revealed that the dye can be used to monitor lymphocyte proliferation, both *in vitro* and *in vivo*, due to the progressive halving of CFSE fluorescence within daughter cells following each cell division. (98).The only limitation is that CFSE at high concentrations can be toxic for cells. However, when CFSE labeling is performed optimally, approximately 7-8 cell divisions (approximately 8 weeks) can be identified before the CFSE fluorescence is too low to be distinguished above the autofluorescence background. Thus CFSE represents an extremely valuable fluorescent dye for immunological studies, allowing lymphocyte proliferation, migration and positioning to be simultaneously monitored.

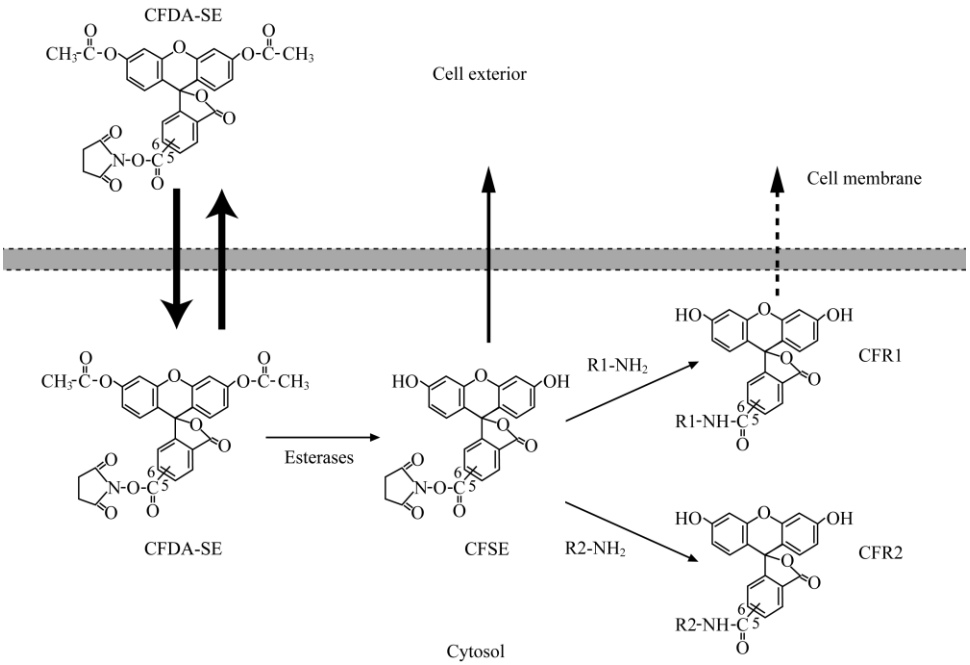

Figure 2.3 Schematic representation of the mechanism involved in the fluorescent labeling of cells using CFDA-SE (99).

First, CFDA-SE is readily taken up by cells. Intracellular esterases, however, can remove the two acetate groups from CFDA-SE to yield fluorescent CFSE. The succinimidyl moiety of CFSE can covalently couple CF to intracellular molecules. In some cases, CF covalently couples to intracellular molecules (R1-NH2) to form conjugates (CFR1) that can still exit from the cell or are rapidly degraded. However, a proportion of CF becomes coupled to long-lived intracellular molecules (R2-NH2) to form conjugates (CFR2) that cannot escape from the cell and thus stable fluorescent labeling of cells is achieved.

Genetically encoded fluorescent proteins such as green fluorescent protein (GFP) have been widely used for cell labeling. GFPs are spontaneous fluorescent proteins isolated from a jellyfish, Aequorea Victoria (100, 101). GFP transduces the blue hemiluminescence of aequorin into green fluorescent light by energy transfer (101). GFPs are typically transfected into the cells via retrovirus, lentivirus, or nonviral approaches (102). Stem cells can also be used from GFP transgenic animals. In comparison with organic dyes, GFPs have a number of advantages

such as better photostability and pH tolerance in addition to longer luminescence time. The biggest advantage is that the presence of GFP means that the cells were alive at the time of sampling because the GFP has to be actively produced by the cell. With other types of labeling, the label could be present in a cell that ingested the labeled cell. However, GFPs suffer from a number of intrinsic deficiencies, such as sensitivity to proteolytic enzymes and overlap with autofluorescence signals, thus making it difficult to track cells *in vivo* (103, 104).

Quantum dots (QDs) can also be used for cell labeling. QDs are small, light-emitting semiconductor nanocrystals, typically in the size range of 2-10 nm (105, 106, 107, 108, 109). QDs are generally composed of atoms from groups II-VI (e.g., CdSe, CdTe, CdS, and ZnSe) or III-V (e.g., InP and InAs) of the periodic table, and are nanoparticles with physical dimensions smaller than the excitation Bohr radius (110, 111). Currently, commercially available QDs are tailored for cell labeling. In contrast to organic dyes or fluorescent proteins, QDs have several distinctive advantages, especially for long-term cell labeling and *in vivo* cell tracking. QDs are generally photo-stable and maintain fluorescent intensity in cell culture for a prolonged time (110, 111, 112).

Magnetic nanoparticles can also be used to label cells. Several noninvasive imaging modalities are available for cell tracking including computed tomography (CT), positron emission tomography (PET), magnetic resonance imaging (MRI), single photon emission computer tomography (SPECT), optical imaging, and ultrasound imaging. Advantages of MRI include its high spatial resolution, widespread availability in most clinics, and that it does not expose the patient to ionizing radiation, which is present in CT, PET, and SPECT. Magnetic nanoparticles can be classified into a few groups—superparamagnetic (Figure 2.4), paramagnetic, ferrimagnetic, and ferromagnetic nanoparticles. Elements such as iron, manganese, and gadolinium have paramagnetic properties due to unpaired electrons and have strong effects on the local magnetic field, which allows them to be utilized as contrast agents for MRI.

Superparamagnetism occurs when the material is composed of very small crystallites (1–10 nm).

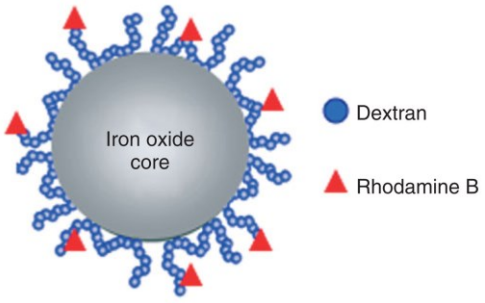

Figure 2.4 Schematic structure of a representative superparamagnetic iron oxide (SPIO) nanoparticle that is composed of an iron oxide core, dextran coating, and rhodamine as fluorescent marker. (113).

2. 6 Different methods of Delivery of stem cells

1. Direct injection: It is possible to transplant the cells directly to the site of injury. One disadvantage with this method is, it is associated with low therapeutic efficacy because of graft rejection by immunologic reaction if non-autologous cells are used. Also, as a consequence of direct tissue trauma resulting from inflammation, cerebral edema and reactive gliosis, this method is associated with low efficacy. However, this method delivers the most cells to a particular site.

2. Cell Delivery Vehicle: A cell delivery vehicle is a matrix that is made from natural or synthetic or combination of the two, which acts a vehicle to carry cells to be transplanted into a human or animal host. There are different types of vehicles (table 2.1) for this purpose, which are commercially available.

Matrix	Origin	Commercial Name
Fibrin	Human Plasma	Tisseel

Collagen I	Human Fibroblast Cells	Vitrocol
Alginate	Seaweed	AlgiMatrix
Crosslinked Hyaluronate	Bacillus subtilis	Hystem
Polyethylene glycol diacrylate (PEGDA)	Synthetic	NA
Self-assembling peptides	Synthetic	HydroMatrix

Table 2.1 Showing different Cell delivery vehicles.

Their structure and composition is designed to overcome the problems associated with immunological issues, low cell density, graft failure attributed to ischemia and finally anoikis (that is, apoptosis induced by lack of correct cell/ECM attachment). Patient to patient variability in terms of desired type of matrix, the type of tissue, the injury size and depth, methodology of delivery of cells and technical challenges like embedding cells within a matrix are the major limitations for their use (114, 115).

3. Intravenous method: If the cells are administered intravenously, they have to make the transition from the venous to arterial system in lungs before they could reach the brain and spinal cord. Several studies have found that the cells after intravenous injection were distributed massively in systemic circulation and get entrapped in peripheral organs such as lungs, liver and spleen (116, 117)

4. Intra-arterial method: Even though intra-arterial route of delivering the cells avoids the problem of crossing the lung into the arterial system, it is associated with microvascular occlusion impeding the cerebral blood flow (118, 119). This may have serious effects such as stroke.

5. Intrathecal route: Mixed results were obtained when cells were injected into the CSF. Intrathecal injection of bone marrow stromal cells attenuated neurologic injury after spinal cord ischemia (120). Intrathecal injection of neuroectodermally converted stem cells in a mouse

model of ALS showed limited intraparenchymal migration and survival thus reducing the therapeutic efficacy (121).

6. Intranasal method: In 2009, it was discovered that eukaryote cells (bone marrow mesenchymal cells or human glioma cells) could be delivered to the brain and spinal cord through the nose (122). The cells were found to migrate through the olfactory mucosa (present in uppermost part of the inside of the nose) to enter the cerebrospinal fluid (CSF) or migrate along axons. Dr. Zwijnenburg, P.J.G and his colleagues (*The journal of Infectious Diseases, 2001)* demonstrated that, application of Hyaluronidase (HU) one hour before the application of the cells to facilitated the delivery of bacteria through the nose. This delivery method was used with some success in an animal model of Parkinson's disease (118).

7. OMPC: Following application of OMPCs, the axons could be regenerated and functional improvement was witnessed in an animal model of spinal cord injury; in hearing loss (123); in hippocampal lesions (124). Olfactory mucosal autografts are proved to be feasible, safe and beneficial in patients with SCI when combined with postoperative rehabilitation (125).

Chapter 3

Pilot Study of Labeling Stem Cells and Intranasal Stem Cells Delivery after Spinal Cord Injury

3.1 Objective and Experimental Design

The objectives of this pilot project were to determine:

1) Toxicity and effectiveness of various doses of CFDA;

2) Potential use of hyaluronidase to improve the effectiveness of intranasal cell delivery;

3) Effectiveness of the nose drop method compared to the tubing method of cell delivery.

After the *in vitro* testing for the CFDA, rats were randomly assigned to the treatment groups illustrated below:

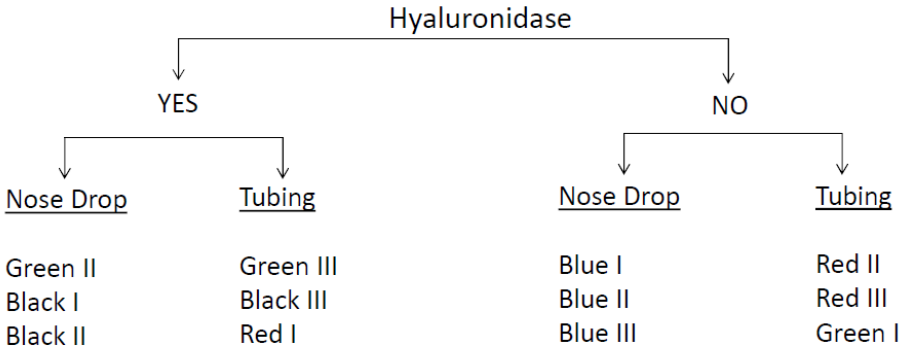

3.2 Materials and Methods:

Rats:

15 Male Lewis rats that were 2 months old (weighing 260-285 gm) were housed in groups of three in polycarbonate cages with corncob bedding, maintained on a 12:12-hr dark:light cycle and given food and water ad libitum. All studies were approved by the

Institutional Animal and Care Use Committee (IACUC) of Wayne State University (Protocol number: A1-08-11). Following surgery, bladders were expressed twice/day until return of bladder function.

OMSC Isolation and Culture:

We have maintained the olfactory mucosal stem cells that were obtained after sacrificing three Lewis rats. To do this, the rat was deeply anesthetized with urethane (2.3 g/kg body weight), then checked at regular intervals to make sure the rat was unresponsive to pain by pinching the toe before sacrificing by cervical dislocation. If necessary, supplementary doses of urethane (0.6 g/kg body weight) were given until the rat was totally unresponsive to toe pinch and had lost the corneal reflex. As soon as the rat stopped breathing and the heart stopped, a bilateral pneumothorax was performed to assure death then the head was decapitated and the skin removed. The head is rinsed with water to remove any loose hairs. Parasagittal cuts (close to the midline on both sides) are made in the snout and part of the skull using a Dremel Moto-tool with a fiberglass reinforced cut-off wheel. The lateral tissue was reflected to expose the medial surface of the nasal cavity. The olfactory mucosa is yellow in color. The olfactory mucosa was rinsed several times with sterile Hank's balanced salt solution (HBSS) then removed and placed in a sterile non-treated tissue culture Petri dish with a drop of HBSS on cold pack. The tissue was minced using scalpels with #15 blades in Hank's balanced salt solution for mechanical dissociation that was followed by the addition of Dispase I and DNAse II and incubated for 30 minutes at 37 degrees Celsius. For further tissue disruption, the mixture was then centrifuged and the pellet formed was resuspended in Accutase and incubated for 30 minutes at 37 degrees Celsius. The pellet formed was resuspended in growth medium consisting of DMEM/F12, B27, Pen/Strep, bFGF, EGF and 10% fetal bovine serum (FBS) overnight. The next day, the cells were plated on a sterile, non-treated tissue culture plate and incubated in an atmosphere of 5% CO_2 at 37 degrees Celsius and fed every 3-4 days with the

growth medium without FBS. Non-treated plates prevent cell adhesion and encourage cell division.

Trypan Blue viability assay:

It is a type of dye exclusion test used to determine the number of viable cells present in a cell suspension. The dye only passes through the membrane of dead cells.

Fluorescent labeling:

Carboxy Fluorescein DiAcetate Succinimidyl Ester (CFDA-SE) labeling: (Invitrogen, Vybrant® CFDA SE Cell Tracer Kit, Eugene, OR). It is a fluorescent cell staining dye. CFDA-SE, due to its acetate groups, is highly cell permeable. CFDA-SE is colorless and non-fluorescent but intracellular esterases in the cytoplasm remove the acetate groups of CFDA and convert the molecule to the fluorescent ester, CFSE, which is retained within cells and covalently coupled, via its succinimidyl group, to intracellular molecules (96). Due to this covalent coupling reaction fluorescent CFSE can be retained within cells for extremely long periods. Also, due to this stable linkage, once incorporated within cells the dye is not transferred to adjacent cells. When CFSE labeling is performed optimally, approximately 7-8 cell divisions can be identified before the CFSE fluorescence is too low to be distinguished above the autofluorescence background.

The stock solution was prepared by mixing the contents of vial A with the contents of vial B to obtain a stock solution at a concentration of 10 mM. The working concentration of the dye varies from 0.5 µM to 25µM. We worked on different concentrations CFDA to finalize the concentration of CFDA to be used for our cells. Initially the experiment was conducted at a working concentration of 10 µM (Experiment A1) and later (Experiment A2) with four different working concentrations: 5, 15, 20 and 25 µM. To do this, initially the stem cell sample (1 million in number) is centrifuged at a rate of 100 rcf for 10 minutes. The pellet is then resuspended in a given concentration of CFDA in 1 ml of PBS. Then the cells are incubated at 37°C, 5% CO2 for 15 minutes. Then they are centrifuged at 100 rcf for 10 minutes, resuspended the pellet in fresh nutrient medium and transferred to Glass chambers (Experiment 1) or to Matrix gel (Experiment

2). In experiment 2, we used 4 different working concentrations of CFDA. These cells are later visualized by fluorescence microscopy using standard fluorescein filter sets at an excitation and emission peaks of 492 nm and 517 nm respectively. We did not see any fluorescence in Experiment 1 using a concentration of 10 µM. In Experiment 2, we detected fluorescence in the sample that had CFDA at 5 µM concentration. We used this concentration in our project.

Fluorescent microscope:

The spinal cord sections were mounted onto the microscope slide, cover slipped with Fluoroshield (Sigma Life Science, St Louis, MO) and examined using a fluorescent microscope using appropriate filters. The green fluorescence indicated those cells which contain cells labeled with CFDA.

Surgical details for inducing SCI using MASCIS impactor:

All the rats were given Buprenex (0.05 mg/kg body weight) 30 minutes before surgery, anesthetized with 5% isoflurane in tube then maintained at 1.5-1.8% with nose cone. Oxygen was maintained at 1.5 lpm. Paralube ointment was applied to eyes and rat was placed on water circulating heating pad. Temperature probe was placed in rectum. Rats were shaved and skin was cleaned with betadine scrub then 70% alcohol three times. Skin incision was made, dissection by planes was performed on spinous processes, detaching the spinotrapezium muscle from bone, laminectomy was done at the level of T9-T10 exposing the meninges. A mild spinal cord injury was induced using MASCIS apparatus by dropping a 10-gram rod from a height of 12.5 mm onto the T9-10 spinal cord exposed by laminectomy. The muscles were sutured using 3-0 suture and the skin was closed using wound clips. Ten ml Lactated Ringers solution was given subcutaneously then anesthesia was stopped. Each rat was kept on oxygen only until it pulled its head out of the nose cone. For a brief period, the animal was placed in a cage without bedding and partially on a water circulating heating pad. It was returned to animal facilities when it was alert. All 12 rats underwent this procedure.

Application of Hyaluronidase (HU) by Nose Drop Method:

100 units of Hyaluronidase (Calbiochem, La Jolla, CA) in a total volume of 24 µl is used. The rats were placed on their sides, a nose drop of 6 µl was carefully placed on one nostril using Hamilton syringe (Hamilton Company, Reno, Nevada) allowing it to be snorted as rats are essentially nose breathers. Another drop of 6 µl is placed on the other side. Procedure is repeated after 5 minutes. All 15 rats received HU.

Application of Cells by Nose Drop Method:

The method for delivery of cells intranasally is essentially same as above. Each rat received one million labeled cells resuspended in 24 µl of sterile PBS. In total, six rats received the cells labeled with CFDA-SE.

Application of Cells Using Tubing method:

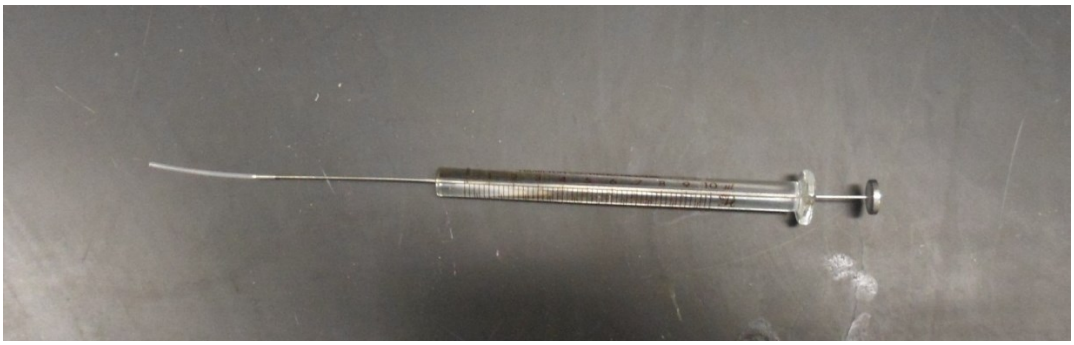

Figure 3.1 Hamilton syringe fitted with polyethylene tube of 23 G caliber and 24 mm in length

Initially 2 dead rats were dissected to determine the length of the tube required to reach olfactory mucosa from external nares. We calculated this to be 24 mm. At the same time, we determined the volume of the fluid (colored using a stain) required to optimally cover the olfactory mucosa (OM) and calculated this to be 6 µl. A flexible polyethylene tube (Intramedic. Clay Adams, Parsippany, NJ) of 23 G caliber and 24 mm length is attached to the end of the Hamilton syringe (Figure 3.1). While advancing in the nasal cavity, care must be taken to avoid damage to nasal mucosa. As it is possible to deliver the cells directly onto olfactory mucosa,

cells reaching the nasopharynx, mouth and trachea can be significantly reduced that deposits the maximum cells onto the OM for absorption.

Preparation of spinal cord sections:

The spinal cord between C3 and T2 level was taken out, rinsed in water then PBS then placed in 4% paraformaldehyde for an hour (for fixation of tissue). The spinal cord was then placed in increasing concentrations of sucrose: 10%, 20%, and 30% until the spinal cord reached equilibrium to prevent freezing artifacts. The spinal cord was cut in the coronal plane at 40 μm on a horizontal sledge type microtome. The specimen were covered in OCT then frozen using dry ice and alcohol in the reservoir of the stage. Sections were collected in 0.1M phosphate buffer, pH 7.2 and refrigerated at 4 degrees Celsius.

Nissl (Cresyl Violet) staining:

Cresyl violet stains the Nissl substance (endoplasmic reticulum and free ribosomes) of a neuron blue. The spinal cord sections were mounted onto microscope slides, passed through a series of solutions: cresyl violet (47 sec), water (brief), Alcohol 50% (41 sec), 75% (41 sec), 95% (41 sec), 100% (41 sec), Histoclear (brief) in that order and then cover-slipped using Histomount. The sections were observed under regular microscope at 5X magnification. The motor neuron cell bodies are visible in the ventral horns of the gray matter as large darkly stained cells.

3.3 RESULTS

We have cultured rat as well human OMPCs. Once a single cell suspension is obtained, culture, numerous cells died in the first few days in culture leaving the stem cells that rapidly divided. The cells were initially rounded but later formed long processes as seen in Figure 3.2

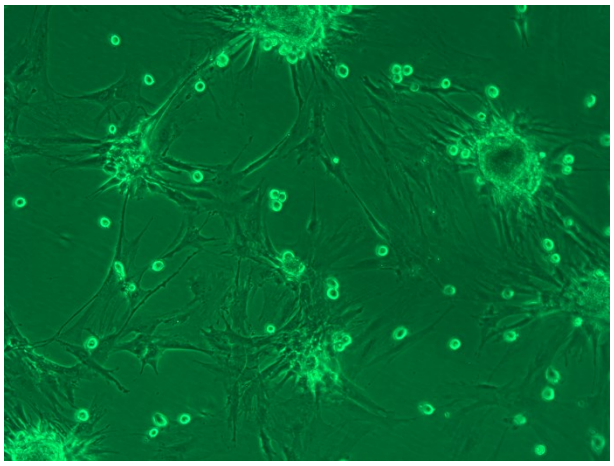

Figure 3.2: Infrared microscopic image showing OMSCs grown *in vitro* after isolation from nasal cavity and after several passages (10X objective)

Twelve rats received cells labeled with CFDA. Six of them received HU one hour prior to cell injection. Among them, three received cells intranasally by the Nose Drop method and other three received cells by the Tubing method. Among the other six rats which did not receive HU, three of them received cells by the Nose Drop method and other three by Tubing method. After three weeks, animals were sacrificed, spinal cords were removed, sections were collected and observed under fluorescent microscopy. We did not observe fluorescence emitted from the labeled cells from any of the sections. So we could not determine which route of cell injection was better. Also we could not determine whether HU has role in enhancing the efficacy of cell injection.

3.4 Discussion and Conclusion:

Initially when we chose 10 μM concentration of CFDA, cells were not alive in the culture. We could not observe any fluorescence emitted from cells in our sections. It is possible that the label might have been toxic to cells. So in the next set of experiments, we chose 4 different concentrations. Among them the cell sample which has received 5 μM concentration of CFDA showed live cells after a week in culture. So we decided to use the same concentration of CFDA

for labeling cells. Even though we checked the cells after a week, we failed to recheck them after another 2 weeks. It is possible that the cells did not survive 3 weeks at this concentration of CFDA. This could be the reason why we did not find any labeled cells when we used a concentration of 10 μM of CFDA. Even with the lower concentration of 5 μM of CFDA, the cells may die after longer periods of time from toxicity of CFDA. We did not evaluate a concentration of less than 5 μM of CFDA.

Chapter 4

Pilot Study Comparing Different Stem Cell Delivery Methods after Motor Neuron Destruction

4.1 Aims and Experimental Design:

The objectives of this project are: 1. To determine if OMPCs reach the injury site in the cervical spinal cord following injection of cells into the CSF of the cisterna magna; 2. To determine whether OMPCs reach the injury site in the spinal cord following intranasal route of cell delivery. Three rats were tested using the limb asymmetry test then injected with CTB-SAP in the motor end plates of the triceps brachii muscle to destroy motor neurons at the spinal level of C6 and C7. One week later the rats were tested in the forelimb asymmetry test to determine if there were any functional deficits. Then stem cells were delivered at 3 weeks after CTB-SAP injection using any one of three methods over a 2 day period (Table 4.1). One week later, the rats were sacrificed and the spinal cord examined for labeled cells.

Rat	Day 1		Day 2	
	Type of cells	**Route of injection**	**Type of cells**	**Route of injection**
Blue I	Labeled	Intrathecal	Unlabeled	Nasal Tubing
Blue II	Unlabeled	Intrathecal	Labeled	Nasal Tubing
Blue III	Labeled	Intraspinal	Unlabeled	Nasal Tubing

Table 4.1: Table showing the details regarding the type of cells injected, route of stem cell injection, and amount of fluorescence emitted from 3 rats.

4.2 Materials and Methods:

Male Lewis rats that were 2 months old (weighing 260-285 gm) were housed in polycarbonate cages with corncob bedding, maintained on a 12:12-hr dark:light cycle and given food and water ad libitum. All studies were approved by the Institutional Animal and Care Use Committee (IACUC) of Wayne State University (Protocol number: A1-08-11).

OMSC Isolation and Culture:

We have maintained the olfactory mucosal stem cells that were previously obtained after sacrificing three Lewis rats. To do this, rats were deeply anesthetized with urethane (2.3 g/kg body weight), they were checked at regular intervals to make sure the rat was unresponsive to pain by pinching the toe. If necessary, supplementary doses of urethane (0.6 g/kg body weight) were given until the rat was totally unresponsive to toe pinch and had lost the corneal reflex. As soon as the rat stopped breathing and the heart stopped, a bilateral pneumothorax was performed to assure death.

When the rat was dead, the head was decapitated and the skin removed. The head is rinsed with water to remove any loose hair. Parasagittal cuts (close to the midline on both sides) are made in the snout and part of the skull using a Dremel Moto-tool with a fiberglass reinforced cut-off wheel. The lateral tissue was reflected to expose the medial surface of the nasal cavity. The olfactory mucosa is yellow in color. The olfactory mucosa was rinsed several times with sterile Hank's balanced salt solution (HBSS) then removed and placed in a sterile non-tissue culture treated Petri dish with a drop of HBSS on cold pack. The tissue was minced using scalpels with #15 blades to mechanically dissociate in Hank's balanced salt solution which is followed by the addition of Dispase I and DNAse II and incubated for 30 minutes at 37 degrees Celsius. For further tissue disruption, the mixture was then centrifuged and the pellet formed was resuspended in Accutase and incubated for 30 minutes at 37 degrees Celsius. The pellet formed was resuspended in growth medium consisting of DMEM/F12, B27, Pen/Strep, bFGF,

EGF and 10% fetal bovine serum (FBS). The cells were plated on a sterile, non-tissue culture treated plate and incubated in an atmosphere of 5% CO_2 in air at 37 degrees Celsius and fed every 3-4 days with the growth medium without FBS.

Trypan Blue Viability Assay:

It is a type of dye exclusion test used to determine the number of viable cells present in a cell suspension.

Fluorescent labeling:

4',6-diamidino-2-phenylindole(DAPI) labeling: (Invitrogen, Molecular Probes, Eugene, OR). It is a nucleic acid stain that binds at rich clusters in the minor groove. The stock solution was prepared by dissolving the contents of one vial (10 mg) in 2 ml of deionized water that results in a concentration of 5 mg/ml. A working concentration of 20 µg/ml is added to each ml of media that contains 1 million cells and incubated overnight. This media is centrifuged at 70 rcf for 5 minutes to obtain the pellet which was resuspended in 24 µl of fresh media for injection for each rat. After the animal is sacrificed, the spinal cord was sectioned. When these sections were viewed under fluorescent microscope, DAPI is observed in nuclei as blue fluorescing spots with an excitation maximum of 358 nm and emission maximum of 461 nm. The number of labeled cells in every third section was counted.

***Surgical details of injecting CTB-SAP*:**

CTB-SAP (Advanced Targeting Systems, San Diego, CA). We followed the surgical procedure originally described by Tosolini and Morris (79) to expose the motor end plates of Triceps brachii muscle. The animals were anesthetized with isoflurane (Baxter Healthcare Corporation, Dearfield, IL; 2–4% in O_2), and the skin area covering the targeted muscles was shaved and cleaned with ethanol. Incisions in the skin were made to expose the muscle of interest. Only the fascial sheaths covering the muscle were removed. The three heads of triceps brachii are located and the location of motor end plate was determined. Then 3 µl of 0.1 % solution of CTB-SAP was injected into the area of the motor end plates. Skin was closed and 10

ml Lactated Ringers solution was given subcutaneously to the rat. When the anesthesia was stopped, the rat was kept on oxygen until it pulled its head out of the nose cone. For a brief period, the animal was placed in a cage without bedding and partially on a water circulating heating pad and was then returned to animal facilities when fully alert.

Delivery Methods:

For intranasal delivery of cells, a detailed description is provided in Section 3.2. Hyaluronidase and tubing was used for this method. For intraspinal injection, the spinal cord was exposed at C6 and C7 by laminectomy and injected. This is the primary location of the motor neurons that innervate the triceps brachii muscle (C6 and C7). A handheld Hamilton syringe with a 26 gauge needle was used to deliver 5 µl (1 million cells) into the spinal cord. For the CSF delivery, a tube is placed by insertion through the atlanto-occipital membrane into the cerebrospinal fluid. A 1-inch midline incision is made on the neck starting at the occipital ridge using a #15 scalpel blade. The head is dorsiflexed and a midline incision is made through the neck musculature. The connective tissue over the atlanto-occipital membrane is removed using fine forceps. A small slit is made in the membrane using a 26-gauge needle. Silicone tubing (1 French, Access Technologies) is inserted and threaded caudally 0.7 cm into the cisterna magna. The tubing is connected to a 50 microliters Hamilton syringe. Five microliters of solution is injected into the CSF over a 15-minute period. Suture is placed through the muscle on both sides of the opening so that the region can be quickly closed when the catheter is to be removed. The catheter is removed 5 minutes after the solution is injected. The muscles are sutured with 4-0 Vicryl then the skin is closed using wound clips. The rat is given 5 cc of saline subcutaneously to compensate for any fluid loss.

Limb-Use Asymmetry:

Figure 4.1 Rat in a glass cylinder while the behavioral test is being administered *(source: Schaar KL, Brenneman MM, Savitz SI - Exp Transl Stroke Med, 2010)*

The limb asymmetry test was developed by Schallert and colleagues (2000) for possible use in focal ischemia, focal cortical lesions, cervical spinal cord injuries and nigrostriatal neurodegeneration. Forelimb use during explorative activity was measured by observing rats in a glass beaker (20 cm diameter and 30 cm height) for about 5 min depending on the degree of movement maintained during the trial (Figure 4.1). Contact the wall by left, right or both forelimbs is recorded and the degree of asymmetry is measured.

Preparation of spinal cord sections:

The spinal cord between C3 and T2 level was taken out, rinsed in water, rinsed in PBS, put in 4% paraformaldehyde for an hour (for fixation of tissue) in that order and then placed in increasing concentrations of sucrose: 10%, 20%, and 30% until the spinal cord reached equilibrium to prevent freezing artifacts. The spinal cord was cut in the coronal plane at 40 μm on horizontal sledge type microtome. The specimens were covered in OCT then frozen using dry ice and alcohol in the reservoir of the stage. Sections were collected in 0.1M phosphate buffer, pH 7.2 and refrigerated at 4 degrees Celsius.

Fluorescent microscope:

The spinal cord sections were mounted onto the microscope slide, sealed with Fluoroshield and cover slips (Sigma Life Science, St Louis, MO) and examined using a fluorescent microscope using appropriate filters. The blue fluorescence indicated those cells which contain nuclei labeled with DAPI.

4.3 RESULTS

This experiment has made us to reconsider the parameters we have used in the study. This time we decided to test new parameters on a small number of animals. As we thought that the CFDA might have been toxic to cells, we tried DAPI for labeling the cells in the subsequent study. Also we decided to use a different injury model in the new study. Our lab has previously used CTB-SAP to selectively kill motor neurons in the spinal cord. The advantage with this method is that the motor neurons on one side of the spinal cord can be destroyed while the other side serves as a control. In such studies, OMPCs were never used to determine if the cells would home to the injury site following an injury created using CTB-SAP. In this study, 3 rats were injured using CTB-SAP and received DAPI labeled cells using 3 different methods.

At one week after injection of CTB-SAP into the muscles of experimental rats, we observed asymmetry in the limb usage, which was confirmed by 'Limb-Use Asymmetry' test. This behavioral test measures the degree of preference for using the unimpaired forelimb for weight shifting purposes during vertical exploratory activities when rat is placed in a glass cylinder. By the end of 3 weeks after injection of neurotoxin, we observed maximum asymmetry in limb usage (Figure 4.2).

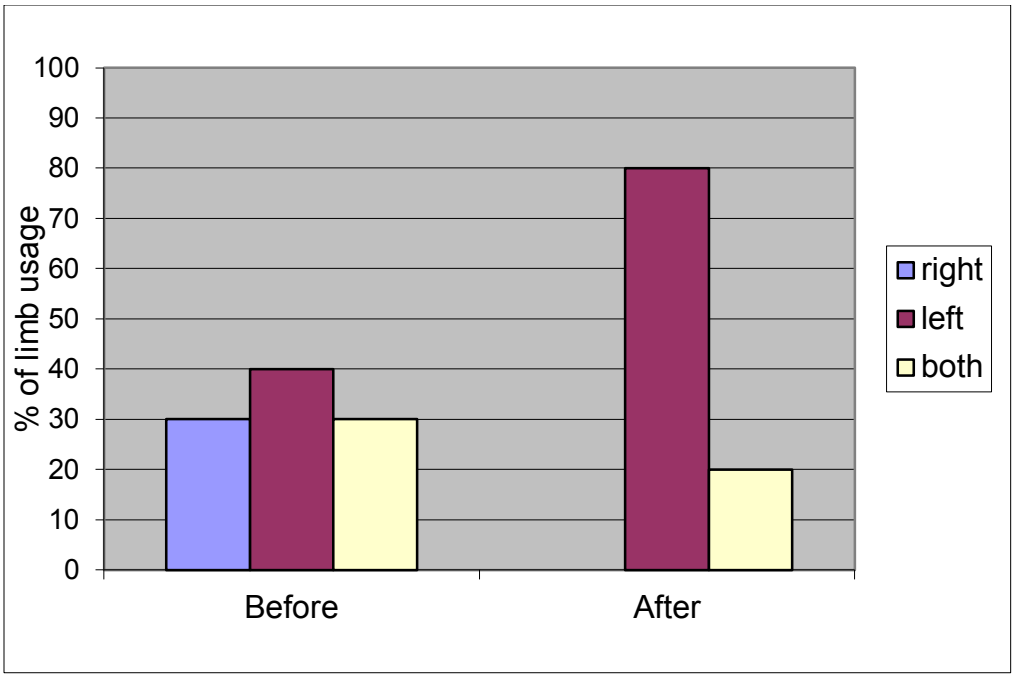

Figure 4.2 Showing the results of Limb-Use Asymmetry test before and after the injection of CTB-SAP

After maximal injury, OMPCs were injected to rats over a period of 2 days. On first day, 2 rats (Blue 1, Blue 3) received labeled cells injected into the CSF and another rat (Blue 2) received cells intraspinally. On the second day, 2 rats (Blue 1, Blue 3) received unlabeled cells intranasally and another rat (Blue 2) received labeled cells intranasally. Each injection consisted of one million cells.

At one week after cell injection, the rats were sacrificed, spinal cords were removed and sectioned using a horizontal sledge microtome at a thickness of 40 µm. Sections were collected in PBS and stored in a refrigerator. From this pool of sections, every third section was chosen for observation. Sections were covered with Fluoroshield and observed under fluorescent microscopy. The fluorescence of DAPI from nucleus of the stem cells would be seen as blue spots dispersed within the tissue (Figure 4.3).

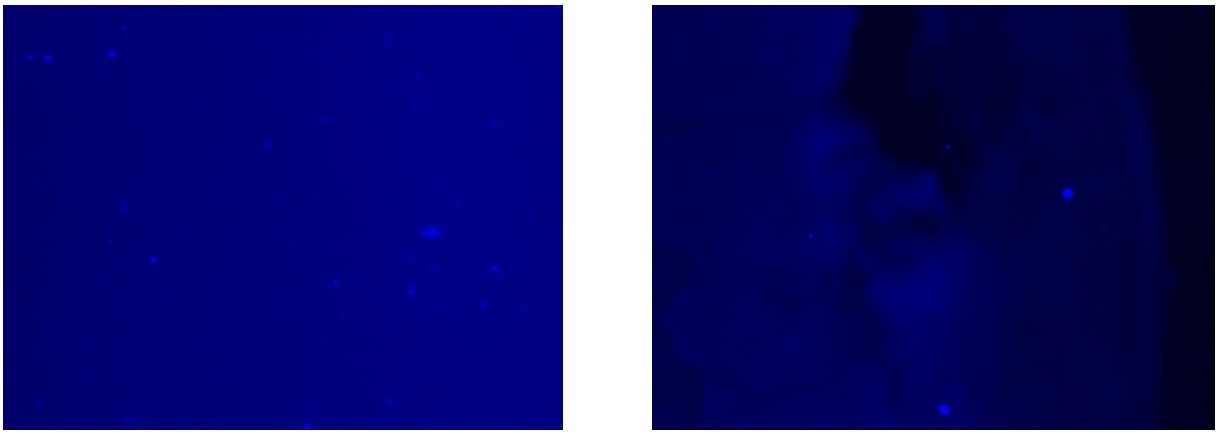

Figure 4.3: Showing the blue fluorescent nuclei dispersed among the spinal cord tissue. These spots indicate the fluorescence emitted from stem cell(s) labeled with DAPI.

We counted the number of such blue nuclei (table 4.2). For this purpose, we randomly selected 3 sections from all the available sections of all the three rats (Blue I, Blue II and Blue III).

Rat	Day 1		Day 2		Fluorescent count
	Type of cells	Route of injection	Type of cells	Route of injection	
Blue I	Labeled	Intrathecal	Unlabeled	Nasal Tubing	104
Blue II	Unlabeled	Intrathecal	Labeled	Nasal Tubing	46
Blue III	Labeled	Intraspinal	Unlabeled	Nasal Tubing	15

Table 4.2: Table showing the details regarding the type of cells injected, route of stem cell injection and number of labeled cells from 3 rats.

We observed highest amount of fluorescence in the rat that received injection of labeled cells into the CSF. Next highest is seen in Blue II which has received labeled cells by tubing

method. The least number of fluorescence labeled cells was seen in Blue III that received labeled cells intraspinally.

From the remaining sections, again every 3rd section was collected, mounted on glass slide, subjected to cresyl violet staining. Then the slides were cover slipped and observed under microscope at 5X magnification. The motor neuron cell bodies were visible in ventral horns of gray matter as large darkly stained cells (Figure. 4.4, 4.5, 4.6). We observed that there were less motor neurons on the side of spinal cord in which the triceps muscle was injected with CTB-SAP compared to the opposite side (Figure. 4.7, 4.8)

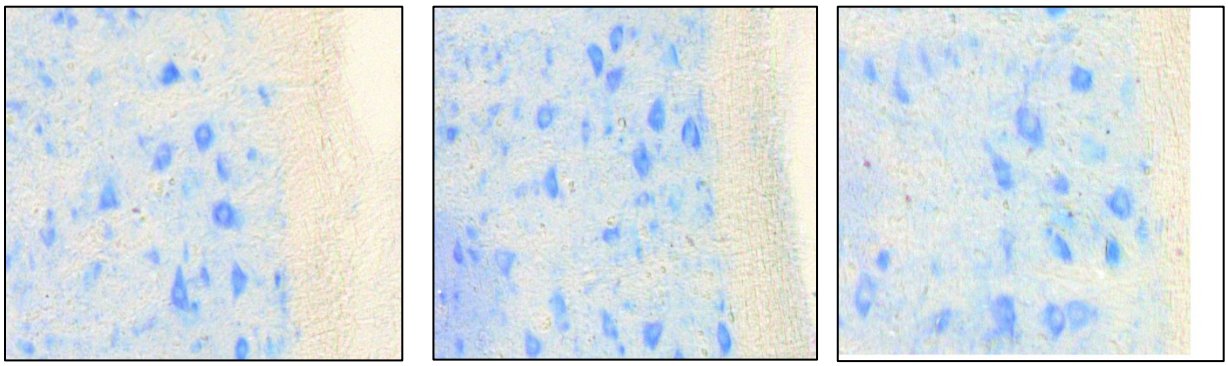

Figure 4.4, 4.5, 4.6: Typical morphology of motor neuron cell bodies visible in ventral horns of gray matter. (blue 1b5, 1b5, 1b5)

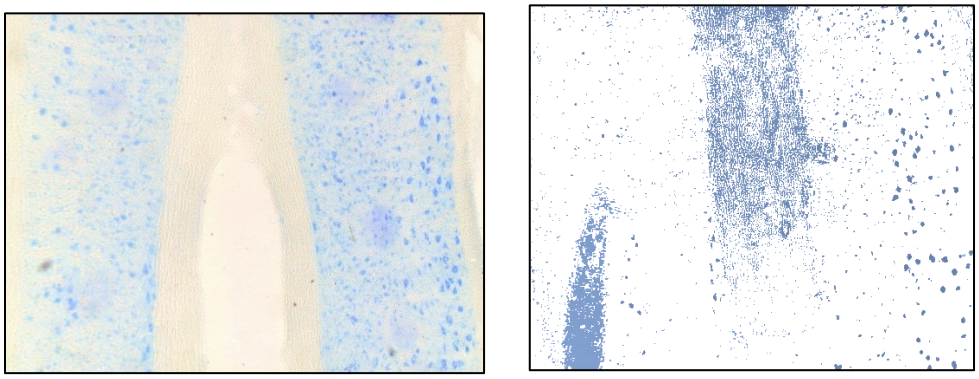

Figure 4.7, 4.8: Less motor neurons are observed on one side of spinal cord compared to the opposite side (blue 1b5, 2c6).

Further, we have also observed that, more number of labeled cells (Figure. 4.9, 4.10) were seen in the area of the spinal cord corresponding to C6 and C7. There were less labeled cells rostrally and caudally compared to the area of injury.

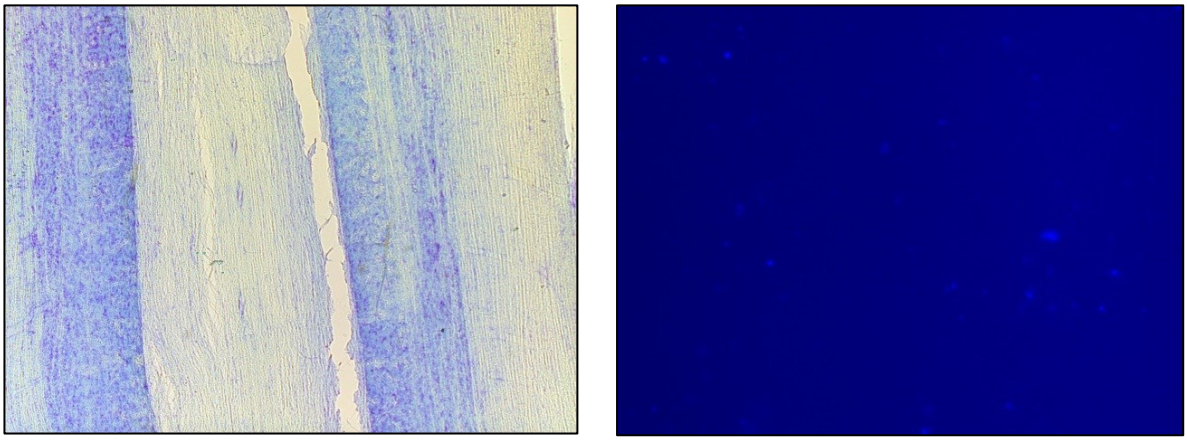

Figure 4.9, 4.10 Showing Cresyl Violet stain and Fluorescent microscopy of the section of spinal cord corresponding to C6 and C7 (blue 1a2, 1a3).

4.4 Discussion and Conclusion:

This study is the first to assess the migration of OMPCs delivered using 3 different methods after SCI induced by intramuscular injection of a neurotoxin that is targeted to spinal motor neurons. The results of the current study are exciting in two aspects. First, DAPI can be successfully used to stain stem cells instead of CFDA without worrying about the toxicity. Second, OMPCs can traverse the olfactory epithelium to primarily reach the CSF as described by Danielyan and colleagues (118). They then migrate to the site of CNS injury, presumably based on cues driven by chemoattractants such as chemokine stromal derived factor 1 (126). The outstanding feature of the present experiment is its simplicity in delivering the stem cells to the central nervous system. The intranasal method is an elegant yet high efficacious way to deliver the stem cells. It is clearly superior to invasive methods of injecting the cells when a disease process demands stem cell injection on multiple occasions over a period of time. Our study was designed to simulate a clinical scenario. Once the stem cells are isolated from the

body, they need to be allowed to grow in culture for a minimum of 2 weeks to expand *ex vivo*. As we injected the cells 3 weeks following injury, our study simulated a clinical scenario.

4.5 Future directions:

Our lab has successfully isolated the OMPCs from rat as well human olfactory tissue; maintained them in conditions that follow FDA guidelines and stored them in liquid nitrogen. In the long term. we aim to optimize the parameters to enhance the efficacy of delivering stem cells to the injured CNS. In this context, my project is significant in terms of modifying the parameters to enhance the efficacy of delivery of cells to the CSF. The materials and methods must be optimized to maximize the delivery of cells to the CSF from each injection and to maximize cell survival *in vivo*. Our finding that stem cells can be delivered intranasally has opened new approaches to optimizing the parameters for therapy with stem cells in spinal cord injuries.

Our observation that DAPI stained cells could be traced at the site of injury will help future researchers determine how long cells would reside at that site and what are their morphologic differentiation once they reach the site of injury.

The current study design needs to be applied on a greater sample size to obtain statistically significant results. As our study design simulates a clinically relevant scenario, this forms the basis for the preclinical trials.

Chapter5

Evaluation of Methylene Blue and Polyethylene Glycol in an Animal Model of Acute Spinal Cord Injury

5.1 Introduction:

Numerous approaches are used in experimental animal studies to develop a treatment for spinal cord injury including stem cells, blocking inhibitors, neurotrophic factors and use of substrate for growth. Morbidity from spinal cord injuries could be significantly reduced if there existed an effective way of fusing the severed axons or inducing the regeneration of axons. The problem of axonal regeneration has attracted neuroscientists for over a century. An alternative approach is re-connecting the severed nerve using chemicals. We explored the usefulness of polyethylene glycol (PEG) that has been used previously to fuse peripheral axons (127). We describe how PEG may be helpful in restoring the neuronal functionality in terms of behavioral improvement in rats with spinal cord injury.

Severed mammalian neurons degenerate within 1-3 days (128). Even though the axonal segments regenerate at a rate of 1-2 mm per day, this process is slow; partial and non-target-oriented leading to a minimal regain of functionality especially following complete cut-severance (129, 130). The rapidity of the plasmalemmal repair following neuronal damage plays a very important role in the regeneration of the neuron. When there is faster repair of plasmalemmal damage, there is quicker neuronal regeneration (57, 131, 132). Normally calcium seals off small holes in crushed axons (crush-severance) or the cut ends of axons in axonal transections (cut-severance) which hinders axonal regeneration. Various calcium-dependent cellular organelles like protein isomers and membrane-bound vesicles accumulate at the cut ends (57). Oxidizing agents like hydrogen peroxide or thimerosal can increase plasmalemmal fusion severely

affecting the regeneration. On the other hand, anti-oxidants like melatonin or methylene blue and toxins like botulinum, befeldin A, or N-ethylmaleimide interfere with vesicle fusion preventing plasmalemmal sealing, thereby greatly enhancing regeneration (133, 134)

In contrast to the slow and incomplete repair mechanisms in mammalian axons, the invertebrates show a rapid and a complete regenerative capacity resulting in fully functional neurons. The possible reasons for this could be, the neuronal outgrowths need to grow only a few millimeters to join the distal end which would not degenerate for weeks to years (135, 136, 137, 138). This very basic idea of preventing accumulation of calcium at the injured axonal ends and finding a way to fuse the cut ends of the neurons together before plasmalemmal repair occurs, is the goal of the present study based on studies done on experiments done on peripheral nerves by Dr. Bittner and colleagues.

Previous studies have demonstrated that application of calcium-free hypotonic saline followed by application of calcium-free hypotonic polyethylene glycol (PEG) prevents accumulation of organelles and rapid sealing of cut ends, respectively (139). *In vitro* studies show that PEG is an axonal fusogen. The present study investigates the potential of this treatment strategy in acute SCI in mammals (rats).

Recent studies by the Bittner's lab found rapid functional repair of cut or crushed nerves using a series of solutions that includes methylene blue (MB) and polyethylene glycol (PEG). We investigated the potential of this treatment strategy in acute spinal cord injury (SCI).

5.2 Polyethylene glycol and Methylene blue:

Below is the schematic diagram (Figure 5.1) to show the effects seen following application of various solutions used during the experiments in peripheral nerve by Bittner and colleagues (139).

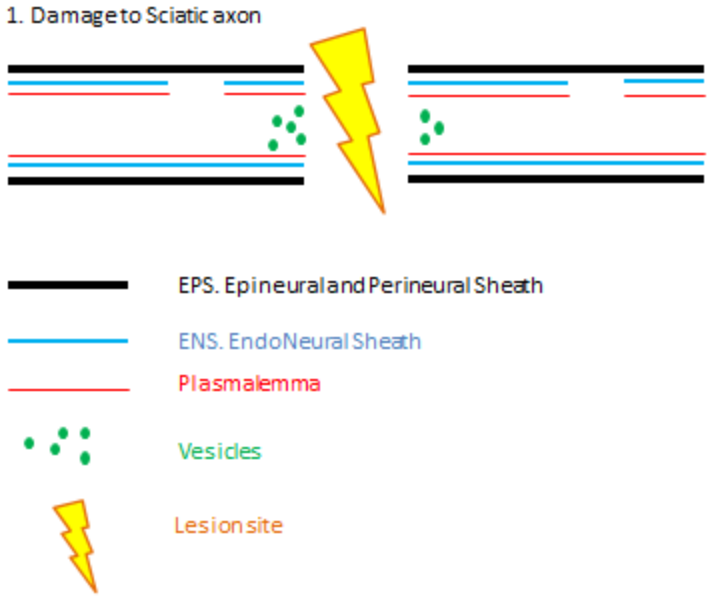

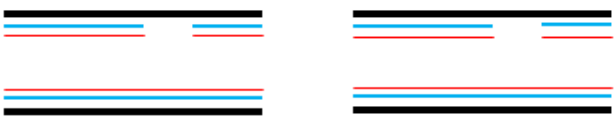

2. Application of Ca^{+2} free hypotonic saline and MB: opens cut ends and expels most vesicles.

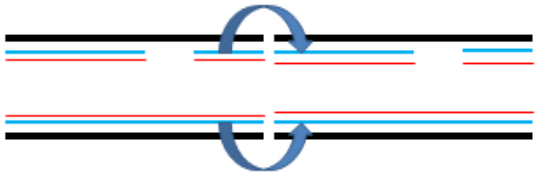

3. Cut ends of axolemmas, ENS and EPS closely re-opposed by micro sutures.

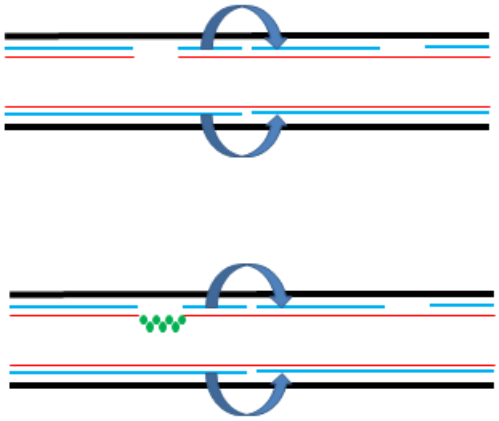

4. Application of Ca^{+2} free hypotonic PEG solution induces membrane fusion (sealing) of some disruptions.

5. Application of Ca^{+2} containing saline: vesicles plug remaining plasmalemmal disruptions.

Figure 5.1: Schematic diagram to show the effects following application of various solutions in peripheral nerve. The diagram illustrates peripheral nerve but the same series of solutions are used in Experiment: 1. 1.When a nerve is cut, there is complete disruption of the axolemma, the epineural and perineural sheath (EPS), and the endoneural sheath (ENS). 2. When calcium free hypotonic saline and Methylene Blue are applied, the cut ends open, expelling the accumulated vesicles. 3. Micro sutures are applied to bring the cut ends of axolemma, EPS and ENS together. 4. Fusion of membranes following application of calcium-free hypotonic PEG solution. 5. Remaining plasmalemmal disruptions are plugged by the application of calcium containing saline.

This sequence of steps applied to rat sciatic nerves restores not only conductance of action potentials and transference of dye across the previous transection but also functional repair when done *in vivo*.

Schematic diagram (Figure 5.2 A, B, C) to illustrate the sequence of effects seen in the formation of membrane vesicles.

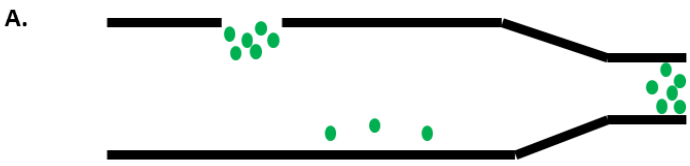

Natural and artificial PEG-induced mechanisms of plasmalemmal repair. Endogenous, Ca^{+2} dependent, vesicle-mediated sealing. (A) Axons seal plasmalemmal damage by Ca^{+2} dependent production of vesicles that form a plug, often at a partially constricted cut end. At small lesions or complete transections, vesicles from nearby undamaged membrane, lysosomes, and/or myelin delaminations migrate, accumulate, and pack tightly at the damage site. These vesicles interact with each other and undamaged membrane to reduce the influx of extracellular Ca^{+2} and other ions until a seal is restored. Complete plasmalemmal repair takes about 24 hr, at which time vesicles are no longer observed at the original lesion site, and a continuous plasmalemma is restored.

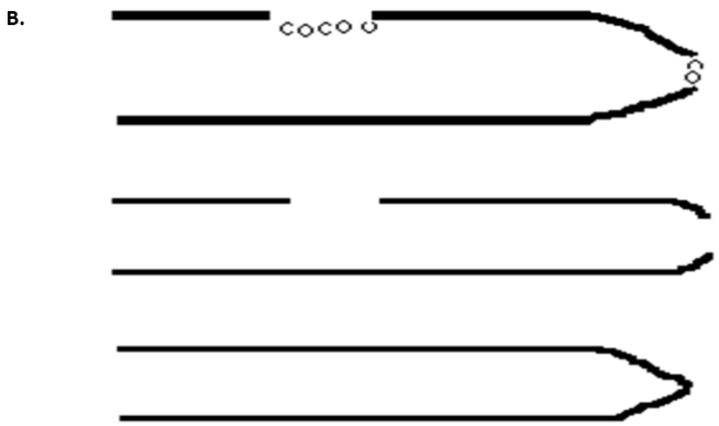

(B) Artificial PEG sealing bypasses all endogenous cellular mechanisms and substances. Application of Calcium free hypotonic saline opens severed ends and expels most vesicles. Application of Calcium free hypotonic PEG solution induces membrane fusion (sealing).

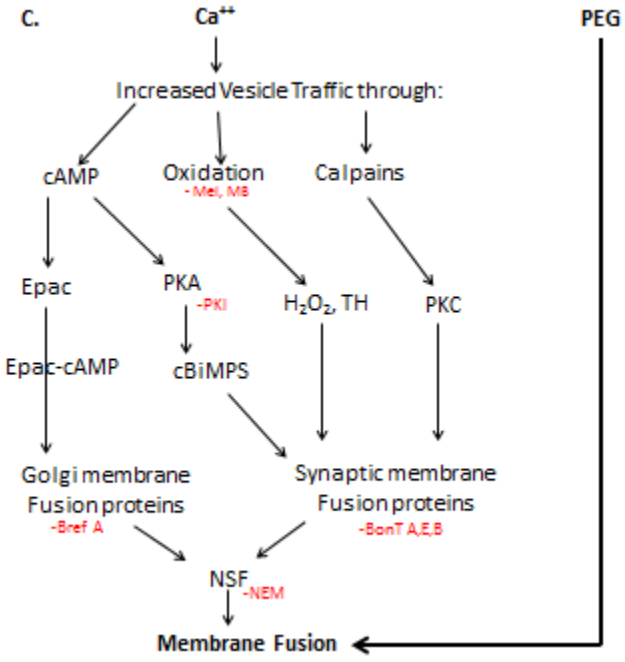

(C) Schematic model of substances in sealing pathways. Bref:- brefeldin A; BoNT:- botulinum toxin-A, -B, or –E; cBiMPS:- Sp-5,6-dichloro-1-b-D-ribofuranosylbenzimidazole- 3 0 , 5 0 – monophosphorothioate; Epac:- exchange protein activated by cAMP; DAG:- diacylglycerol; NEM:- N-ethylmaleimide; NSF:- N-ethylmaleimide-sensitive factor; PKA, PKC:- phosphokinases A and C. As previously described, endogenous, naturally-occurring plasmalemmal sealing requires various proteins, many of whose isomers are Ca^{+2} dependent and involved in membrane fusion at synapses or in the Golgi apparatus such as synaptobrevin, syntaxin, synaptophilin, synaptotagmin, calpains, tripartite motif (TRIM) proteins, PKA, and PKC. Increasing cAMP concentration or specifically activating PKA or Epac via target-specific cAMP analogs produce similar increases in plasmalemmal sealing. Plasmalemmal sealing is decreased by antioxidants such as MB or MEL. That is, plasmalemmal sealing involves redundant, parallel pathways initiated by Ca^{+2} influx. Furthermore, data from over 20 invertebrate and vertebrate preparations (including B104 cells) show that isomers of the same proteins, pathways, and vesicle interactions are likely involved in plasmalemmal sealing of all

eukaryotic cells, indicating that such proteins in eukaryotes evolved to repair plasmalemmal damage (139).

Cellular/Molecular Effects and Rationale in PEG Fusion for the Use of Ca^{2+} -free Hypotonic saline, MB, PEG, and Ca^{+2} -containing isotonic saline

Calcium-free hypotonic saline: In calcium containing isotonic saline, the cut ends of the invertebrate giant axons partially collapse. Brightfield and confocal microscopy have confirmed that these ends open up fully and expel axoplasm containing vesicles in the calcium-free hypotonic saline. Electron microscopy shows that the vesicles get disintegrated (140). Giant axons when cut-severed, take up dye in calcium-free saline and do not take up dye in calcium-containing isotonic saline (139). Dr. Spaeth and colleagues have shown that vesicles form, accumulate and seal the partially collapsed cut ends in calcium-free isotonic saline (134,139).

Methylene Blue Previous studies have shown that the sealing mechanisms operating endogenously are similar in all eukaryotic cells including the roles of calcium and proteins and other substances in various pathways that promote sealing, pathways that are activated by cytoplasmic oxidation (139). Results obtained from *in vivo* experiments on invertebrate axons, sea urchin ova, mammalian axons and non-neural mammalian cells show that the natural process of plasmalemmal sealing requires various proteins (139). Many of them are activated by calcium and have isomers that are involved in membrane fusion in synapses or Golgi apparatus. such as synaptobrevin, syntaxin, synaptophilin, synaptotagmin, calpains, TRIM proteins, PKA, and PKC. Plasmalemmal sealing is diminished by antioxidants like MB and promoted by oxidants like H_2O_2 . Sealing is also enhanced by PKA and EPac activated by cAMP. Antioxidants like MB when applied before PEG application would decrease sealing and help to maintain the patency of axonal ends and free of vesicles and which may possibly enhance PEG-fusion and PEG-sealing.

PEG: As illustrated in above Figures, the results suggest that the PEG bypasses endogenous repair mechanisms by removing waters of hydration at the closely apposing membranes at cut axonal ends and also small holes, thereby allowing membrane lipids of plasmalemmal leaflets to collapse, fuse and seal the cut ends. For instance, none of the chemicals listed above that are implicated in endogenous sealing, including calcium, affects the PEG-sealing mechanism of B104 cells *in vitro* or *ex vivo* (rat sciatic axons). Also, sealing probability increases sigmoidally from 0% to 100% with increasing concentrations of PEG as it could be expected for a substance that directly induces plasmalemmal fusion.

Depending on the concentration and duration of its application., PEG can be used either to fuse or to disrupt the plasmalemma. For instance, lower PEG concentrations applied for 1-2 min *in vitro* seals open axonal ends which do have not closely apposing axonal ends (139). On the other hand, higher concentrations of PEG applied for the same duration of time on B104 cells have deleterious effects. Also, when PEG was applied for more than 3 minutes, PEG-induced fusion was reduced. A PEG concentration of about 50 mM optimally reconnect the crush-severed axons *in vivo* (139).

Calcium-containing isotonic saline: Calcium containing isotonic saline, when applied following the application of PEG, sealed the remaining holes in the severed sciatic axons (141). These experiments have also proved that calcium initiates the formation, accumulation and fusion of vesicles to seal the damaged plasmalemma in eukaryotes, including rats. In summary, PEG-fusion protocols rely on the endogenous cellular mechanisms that are initiated by calcium influx. Following calcium influx, calcium in turn activates other intracellular proteins that act in parallel to bring about the common effect. Such endogenous mechanisms may involve vesicles and membrane interactions that will take minutes to have their full effect. On the other hand, PEG helps to open the vesicle-free cut ends bypassing these endogenous cellular mechanisms to directly produce membrane fusion. To note, this artificial fusion mechanism takes less than a second to complete the process. The data suggest that PEG induces its membrane fusion effect

at concentrations of 5-50 mM that are not harmful to cells in culture when exposed to such concentrations.

5.3 Materials and Methods:

Rats:

Male adult Lewis rats which were 2 months old, weighing 260-285 gm were housed in groups of three in polycarbonate cages with corncob bedding, maintained on a 12:12-hr dark:light cycle and given food and water ad libitum. All studies were approved by the Institutional Animal and Care Use Committee (IACUC) of Wayne State University (Protocol number: A1-08-11). Following surgery, bladders were expressed twice/day until return of function.

The MASCIS impactor:

The MASCIS Impactor (NYU devise) is a device designed to deliver graded reproducible spinal cord contusions in rats. It is a part of a well-defined rodent spinal cord injury model that is used in many laboratories around the world. Most of the recommended procedures for the Impactor are based on experience with the model and work done by the Multicenter Animal Spinal Cord Injury Study (MASCIS). The MASCIS Impactor, formerly called the NYU Impactor, was developed in 1991 by Drs. John Gruner, Carl Mason, and Wise Young. Using the device, a mild SCI was induced by dropping a 10-gram rod from a height of 12.5 mm onto the dural surface of the TV9-10 spinal cord exposed by laminectomy.

Surgical procedure:

All the rats were given Buprenex (0.05 mg/kg bw) 30 minutes before surgery, anesthetized with 5% isoflurane in tube then maintained at 1.5-1.8% with nose cone. Oxygen was maintained at 1.5 lpm.. Paralube ointment was applied to the eyes and the rat was placed on a water circulating heating pad. A temperature probe was placed in the rectum. Rats were shaved and the skin was cleaned with a betadine scrub followed by 70% alcohol three times. A

skin incision was made, dissection by planes was performed on spinous processes, detaching the spinotrapezium muscle from bone, and a laminectomy was done at the level of TV9-10 exposing the meninges. Injury was induced using MASCIS apparatus then the dura was opened immediately and a series of solutions were applied to the exposed spinal cord as described below. The dura was closed and muscles sutured using 3-0 suture. The skin was closed with wound clips. Then 10 ml Lactated Ringers solution was given subcutaneously and isoflurane was discontinued. The rat was kept on oxygen until it pulled its head out of the nose cone. For a brief period, the animal was placed in a cage without bedding and partially on a water-circulating heating pad until it was alert. The rat was then returned to animal facilities.

Chemicals used:

12 rats were divided randomly into 2 groups (Group 1 & Group 2) based on whether they receive PEG or not. Group 1 received:

1) calcium-free saline for x minutes
2) Methylene Blue (MB) (100 μM) in hypotonic calcium-free saline for 3 minutes
3) PEG for 2 minutes (500 mM 2 kDa)
4) Krebs with calcium for 2 minutes

Behavioral tests:

Basso, Beattie and Bresnahan (BBB) score test: It is an efficient and unambiguous locomotor rating scale used to assess recovery following contusion injury in rat spinal cord. The scores are based on the normal recovery of rats with a mild spinal cord injury.

Figure 5.3 Basso, Beattie and Bresnahan (BBB) test

The rats were trained prior to surgery to move in an open field which is a molded plastic circular container with a non-slippery floor. Rats are allowed to move freely and are scored during 4 minutes by the observer for their ability to use their hind limbs, joint movements, paw placement, and weight support and forelimb-hindlimb coordination. Complete paralysis scores '0' and normal locomotion '21'. Following 7 days of surgery, rats were assessed weekly by a 'blinded' evaluator for 5 weeks.

Von Frey filaments: These filaments are used to assess the mechanical hypersensitivity (force of <18 g to elicit hind-paw withdrawal) of the hind limbs to innocuous stimuli. Rat would be placed in a transparent plexiglass box (22 x 16 x 12 cm) on a metal mesh floor, animals were allowed to acclimatize for 15 min or until exploratory behavior ceases. Von Frey filaments applied manually to the mid plantar surface of hind paw in a graded fashion (1, 2, 4, 6, 8, 10, 15, 26, 60, and 100 gm) and the withdrawal threshold was noted every week for 3 weeks.

Hargreaves device: Infrared noxious heat stimulus is used to assess the thermal hyperalgesia (latency of <8 s to elicit hind-paw withdrawal). Animals were placed in a transparent plexiglass box (22 x 16 x 12 cm) with a dry glass floor, rats were allowed to acclimatize for 15 min or until exploratory behavior ceases. A beam of radiant heat at a constant temperature (46^0 C) and

wavelength (50 nm) was applied to the mid plantar surface of the paw. The time required to withdraw the hind limb was noted. As there is an automatic cut-off at 21 sec, there is no risk of thermal injury to the skin. This test was conducted weekly for 5 weeks.

Statistical analysis:

The statistical analysis was conducted using two way ANOVA with Bonferroni post-test.

5.4 Results:

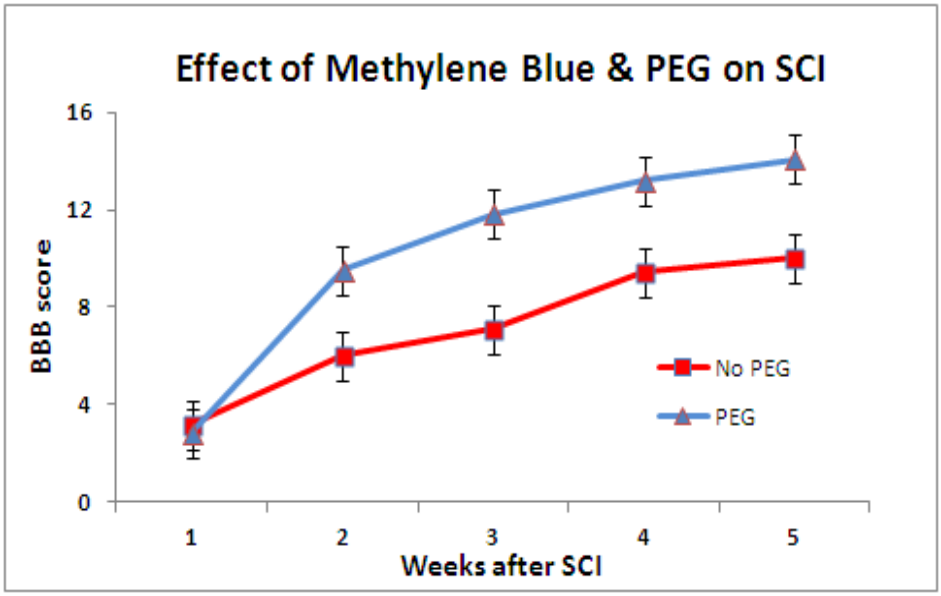

Figure 5.4 Effect of Methylene Blue and PEG on Spinal Cord Injury

In the first week after injury, the mean BBB score of the vehicle=treated group (3.8±1.32 SEM) was higher than the PEG treated group (2.83±0.91 SEM). However at 2 to 5 weeks after injury, the mean scores of PEG treated group was 3-4 points higher than the vehicle treated group and were significantly different at 3 weeks after injury ($p<0.05$). Using a two-way ANOVA with Bonferroni post-test, the curves were statistically different ($p<0.0001$). Results from von Frey and thermal plantar testing appeared to be quite variable between the 2 sides and across time in a given animal even when care was taken to target the exact middle of the pads of the hind paws. There was no significant difference between the 2 groups in these tests.

5.5 Conclusion :

The significant functional improvement in BBB scores as a result of using a series of solutions that contain PEG and methylene blue is encouraging. Clinical translation may be eventually feasible using methods developed to extend the time to axonal fusion using cyclosporine, decreased temperatures or other methods (141). Clinical feasibility is also enhanced because all of the solutions developed for maximal axonal fusion are already FDA approved.

5.6 Future directions:

Overcoming certain technical difficulties such as quick removal of the dura after injury may improve results even more. Also, a study need to be done to evaluate the efficacy when PEG is combined with intraspinal injection of stem cells for spinal cord injuries.

REFERENCES:

1. Rexed, B. (1954) A cytoarchitectonic atlas of the spinal cord in the cat. *J comp neurol*. **100**, 297.
2. Rexed, B. (1964) Some aspects of the cytoarchitectonics and synaptology of the spinal cord. *Prog brain res*. **11**, 58.
3. Rathelot, J.A., Strick, P.L. (2009) Subdivisions of primary motor cortex based on cortico-motoneuronal cells. Proc Natl Acad Sci USA. **106**, 918.
4. Abdel-Azim, M., Sullivan, M., Yalla, S.V. (1991) Disorders of bladder function in spinal cord disease. *Neurol clin.* **9**, 727.
5. Baker, A. B. (1965) Spinal cord localization. *J Lancet*. **85**, 269-274.
6. Wagner, R., Jagoda, A. (1997) Spinal cord syndromes. *Emerg med clin north am* **15,** 699.
7. Biglioli, P., Roberto, M., Cannata, A., (2004) Upper and lower spinal cord blood supply: the continuity of the anterior spinal artery and the relevance of the lumbar arteries. *J Thorac Cardiovasc Surg.* **127,** 1188.
8. Gillilan, L.A. (1956) The arterial blood supply of the human spinal cord. *J Comp Neurol. **110,** 75-103.*
9. Kawaharada, N., Morishita, K., Hyodoh, H., (2004) Magnetic resonance angiographic localization of the artery of Adamkiewicz for spinal cord blood supply. *Ann Thorac Surg.* **78,** 846.
10. Lasjaunias, P., Vallee, B., Person, H., (1985) The lateral spinal artery of the upper cervical spinal cord. Anatomy, normal variations, and angiographic aspects. *J Neurosurg*. **63,** 235.
11. McCormick, P.C., Stein, B.M. (1990) Functional anatomy of the spinal cord and related structures. *Neurosurg Clin N Am.* **1**, 469.

12. NINDS: National Institute of Neurological Disorders and Stroke. Spinal cord injury: Emerging concepts. (Sept 30 – Oct 1, 1996). http://www.ninds.nih.gov/news_and_events/proceedings/sci_report.htm

13. The National Spinal Cord Injury Statistical Center. http://www.spinalcord.uab.edu/show.asp?durki=21446 (Accessed on May 11, 2007)

14. Spinal Cord Injury facts and figures at a glance, National Spinal Cord Injury statistical center, Birmingham, Alabama. Feb. 2012.

15. Ackery, A., Tator, C., Krassioukov, A. (2004) A global perspective on spinal cord injury epidemiology. *J Neurotrauma.* **21,** 1355.

16. Canadian Paraplegic Association. Ottawa, ON, Canada. http://www.canparaplegic.org/en/SCI_Facts_67/items/6.html

17. Spinal cord injury: National Institute of Neurological Disorders and Stroke. Spinal cord injury: Emerging concepts. (Sept 30 – Oct 1, 1996). http://www.ninds.nih.gov/news_and_events/proceedings/sci_report.htm

18. Sekhon, L.H., Fehlings, M.G. (2001) Epidemiology, demographics, and pathophysiology of acute spinal cord injury. *Spine.* **26**:S2.

19. Vitale, M.G., Goss, J.M., Matsumoto, H., Roye, D.P. Jr. (2006) Epidemiology of pediatric spinal cord injury in the United States: years 1997 and 2000. *J Pediatr Orthop* **26,** 745.

20. Myers, E.R., Wilson, S.E. (1997) Biomechanics of osteoporosis and vertebral fracture. *Spine.* (Phila Pa 1976). **22,** 25S-31S.

21. Janssen, L., Hansebout, R.R. (1989) Pathogenesis of spinal cord injury and newer treatments. A review. *Spine.* **14**, 23.

22. Fehlings, M.G., Perrin, R.G. (2005) The role and timing of early decompression for cervical spinal cord injury: update with a review of recent clinical evidence. *Injury.* **36 (2),** B13.

23. Tator, C.H. (1995) Update on the pathophysiology and pathology of acute spinal cord injury. *Brain Pathol.* **5**:407.

24. Horiuchi, D., Barkus, R. V., Pilling, A. D., Gassman, A., and Saxton, W. M. (2005). APLIP1, a kinesin binding JIP-1/JNK scaffold protein, influences the axonal transport of both vesicles and mitochondria in drosophila. *Curr.Bio.* **15,** 2137-2141

25. Hurlbert, R. J. (2001). The role of steroids in acute spinal cord injury: an evidence-based analysis. *Spin*. **26**, S39–S46.

26. Hurlbert, R. J. (2000). Methylprednisolone for acute spinal cord injury: an inappropriate standard of care. *J Neurosur*. **93**, 1–7.

27. Lee, J. K., Geoffroy, C. G., Chan, A. F., Tolentino, K. E., Crawford, M. J., Leal, M. A., et al.(2010). Assessing spinal axon regeneration and sprouting in Nogo-, MAG-, and OMgp-deficient mice. *Neuron* **66**, 663–670.

28. Schnell, L., & Schwab, M. E. (1990) Axonal regeneration in the rat spinal cord produced by an antibody against myelin-associated neurite growth inhibitors. *Nature***.** **343**,269–272.

29. Liebscher, T., Schnell, L., Schnell, D., Scholl, J., Schneider, R., Gullo, M., (2005). Nogo-A antibody improves regeneration and locomotion of spinal cord-injured rats. *Ann Neurol* **58**,706–719.

30. Lehmann, M., Fournier, A., Selles-Navarro, I., Dergham, P., Sebok, A., Leclerc, N., et al. (1999) Inactivation of Rho signaling pathway promotes CNS axon regeneration. *J Neurosci*. **19**, 7537–7547.

31. Boato, F., Hendrix, S., Huelsenbeck, S. C., Hofmann, F., Grosse, G., Djalali, S., et al. (2010) C3 peptide enhances recovery from spinal cord injury by improved regenerative growth of descending fiber tracts. *J Cell Sci*. **123**, 1652–1662.

32. Kaneko, S., Iwanami, A., Nakamura, M., Kishino, A., Kikuchi, K., Shibata, S., Okano, H.J., Ikegami, T., Moriya, A., Konishi, O., Nakayama, C., Kumagai, K., Kimura, T.,

Sato, Y., Goshima, Y., Taniguchi, M., Ito, M., He, Z., Toyama, Y., Okano, H. (2006) A selective Sema3A inhibitor enhances regenerative responses and functional recovery of the injured spinal cord. *Nat Med.* **12(12),**1380-9.

33. Fawcett, J. W., & Asher, R. A. (1999). The glial scar and central nervous system repair. *Brain Res Bulletin*. **49**, 377–391.

34. Fitch, M. T., & Silver, J. (1999). In M. H. Tuszynski, & J. H. Kordower (Eds.), CNS Regeneration: Basic Science and Clinical Advances (pp. 55–88). San Diego: Academic.

35. Bradbury, E., Moon, L. D. F., Popat, R. J., King, V. R., Bennett, G. S., Patel, P. N., et al. (2002). Chondroitinase ABC promotes functional recovery after spinal cord injury. *Nature.* **416**, 636–640.

36. Ramón-Cueto, A., Cordero, M. I., Santos-Benito, F. F., & Avila, J. (2000). Functional recovery of paraplegic rats and motor axon regeneration in their spinal cords by olfactory ensheathing glia. *Neuro.* **25**, 425–435.

37. Cizkova, D., Novotna, I., Slovinska, L., Vanicky, I., Jergova, S., Rosocha, J., et al. (in press). Repetitive intrathecal catheter delivery of bone marrow mesenchymal stromal cells improves functional recovery in a rat model of contusive spinal cord injury. *J Neurotrauma Epub.* ahead of print.

38. Neuhuber, B., Timothy Himes, B., Shumsky, J. S., Gallo, G., & Fischer, I. (2005). Axon growth and recovery of function supported by human bone marrow stromal cells in the injured spinal cord exhibit donor variations. *Brain Res*. **1035**, 73–85.

39. Xiao, M., Klueber, K.M., Zhou, J., Guo, Z., Lu, C., Wang, H., Roisen, F.J. (2007) Human adult olfactory neural progenitors promote axotomized rubrospinal tract axonal reinnervation and locomotor recovery. Neurobiol dis. 26, 363-374

40. Cummings, B. J., Uchida, N., Tamaki, S. J., Salazar, D. L., Hooshmand, M., Summers, R., et al. (2005). Human neural stem cells differentiate and promote locomotor recovery in spinal cord-injured mice. Proc Natl Acad Sci U S A. 102, 14069–14074.

41. Liang, P., Jin, L. H., Liang, T., Liu, E. Z., & Zhao, S. G. (2006). Human neural stem cells promote corticospinal axons regeneration and synapse reformation in injured spinal cord of rats. *Chin Med J Engl Ed*. **119**, 1331–1338.

42. Liang, P., Jin, L. H., Liang, T., Liu, E. Z., & Zhao, S. G. (2006). Human neural stem cells promote corticospinal axons regeneration and synapse reformation in injured spinal cord of rats. *Chin Med J Engl Ed*. **119**, 1331–1338.

43. Ichim, T., Riordan, N.H., Stroncek, D.F. (2011) The king is dead, long live the king: entering a new era of stem cell research and clinical development. *J Transl Med.* **20(9)**, 218.

44. Yamanaka, S. (2012) Induced Pluripotent Stem Cells: Past, Present, and Future. *Cell Stem Cell*. **10,** 678-84.

45. Van der Kooy, D., Weiss, S. (2000). Why stem cells?. *Science*. 287, 1439–41.

46. Gage, F.H. (1998) Cell therapy. *Nature.* 392, 18–24.

47. Blau, H.M., Brazelton, T.R., Weimann, J.M. (2001) The evolving concept of a stem cell: entity or function. *Cell.* **105,** 829–41.

48. Brustle, O., Spiro, A.C., Karram, K. (1997) In vitro-generated neuronal precursors participate In mammalian brain development. *Proc Natl Acad Sci.* **94,** 14809–14.

49. Kuhn, H.G., Winkler, J., Kempermann, G. (1997) EGF and FGF-2 have different effects on neuronal progenitors in the adult rat brain. *J Neuroscience*. **17,** 5820–9.

50. Romero-Ramos, M., Vourch, P., Young, H.E. (2002) Neuronal differentiation of stem cells isolated from adult muscle. *J Neurosci Res*. **15,** 3999–4002.

51. Woodbury, D., Schwarz, E.J., Prokop, D.J. (2000) Adult rat and human bone marrow stromal cells differentiate into neurons. *J Neurosci Res.* **61,** 364–70.

52. Rathjen, J., Haines, B.P., Hudson, K.M. (2002) Directed differentiation of pluripotent cells to neural lineages: homogeneous formation and differentiation of a neuroectoderm population. *Development.* **129,** 2649–61.

53. Reubinoff, B.E., Itsykson, P., Turetsky, T. (2001) Neural progenitors from human embryonic stem cells. *Nat Biotechnol*. **19,** 1134–40.

54. Lanza, D.C., Deem, D.A., Doty, R.L., Moran, D., Crawford, D., Rowley, J.C., Sajjadian, A., Kennedy, D.W. (1994) The effect of human olfactory biopsy on olfaction: A preliminary report. *Laryngoscope*. **104**:837–840.

55. Graziadei, P.P.C., Kaplan, M.S., Graziadei, M., Bernstein, J.J. (1980) Neurogenesis of sensory neurons in the primate olfactory system after section of the fila olfactoria. *Brain Res.* **186**:289–300.

56. Schwob, J.E., Youngentob, S.L., Mezza, R.C. (1995) Reconstitution of the rat olfactory epithelium after methyl bromide-induced lesion. *J Comp Neurol.* **359,** 15–37.

57. Roisen, F.J., Klueber, K.M., Lu, C.L., Hatcher, L.M., Dozier, A., Shields, C.B., Maguire, S. (2001) Adult human olfactory stem cells. *Brain Research*. **890(1),** 11-22.

58. Calof, A.L., Chikaraishi, D.M. (1989) Analysis of neurogenesis in a mammalian neuroepithelium: proliferation and differentiation of an olfactory neuron precursor in vitro. *Neuron.* **3,** 115-127.

59. Graziadei, G.A., Graziadei, P.P. (1979) Neurogenesis and neuron regeneration in the olfactory system of mammals. II. Degeneration and reconstitution of the olfactory sensory neurons after axotomy. *J Neurocytol*. **8,**197–213.

60. MacDonald, K.P., Murrell, W.G., Bartlett, P.F., Bushell, G.R., Mackay-Sim, A. (1996) FGF2 promotes neuronal differentiation in explant cultures of adult and embryonic mouse olfactory epithelium. *J Neurosci Res*. **44**, 27–39.

61. Mackay-Sim, A., Kittel, P.W. (1991) On the Life Span of Olfactory Receptor Neurons. *Eur. J Neurosci.* **3,** 209-215.

62. Mahanthappa, N.K., Schwarting, G.A. (1993) Peptide growth factor control of olfactory neurogenesis and neuron survival in vitro: roles of EGF and TGF-beta s. *Neuron*. **10,** 293-305.

63. Newman, M.P., Feron, F., Mackay-Sim, A. (2000) Growth factor regulation of neurogenesis in adult olfactory epithelium. *Neuroscience*. **99**, 343-350.

64. Pixley SK. (1992). CNS glial cells support in vitro survival, division, and differentiation of dissociated olfactory neuronal progenitor cells. *Neuron.* **8,** 1191–1204.

65. Kopp, H. G., Avecilla, S. T., Hooper, A. T., Rafii, S. (2005) The bone marrow vascular niche: home of HSC differentiation and mobilization. *Physiology (Bethesda)* **20**, 349–356.

66. Magnon, C., and Frenette, P.S., Hematopoietic stem cell trafficking (July 14, 2008) StemBook, ed. The Stem Cell Research Community, StemBook, doi/10.3824/stembook. 1.8.1, http://www.stembook.org.

67. Kelly, A.D., Candace, L.F. (2011) Contusion Models of Spinal Cord Injury in Rats. *Neuromethods*, **62**, 345-362

68. Anderson, K.D., Sharp, K.G., Steward, O. (2009) Bilateral cervical contusion spinal cord injury in rats. *Exp. Neurol*. **220(1)**, 9-22

69. Nottingham, S.A., Springer, J.E. (2003) Temporal and spatial distribution of activated caspase-3 after subdural kainic acid infusions in rat spinal cord. *J Comp Neurol.* **464,** 463-471.

70. Sun, H., Kawahara, Y., Ito, K., Kanazawa, I., Kwak, S. (2006) Slow and selective death of spinal motor neurons in vivo by intrathecal infusion of kainic acid: Implications for AMPA receptor-mediated excitotoxicity in ALS. *J Neurochem* **98**, 782-791.

71. Bao, F., DeWitt, D.S., Prough, D.S., Liu, D. (2003) Peroxynitrite generated in the rat spinal cord induces oxidation and nitration of proteins: Reduction by Mn (III) tetrakis (4-benzoic acid) porphyrin. *J Neurosci Res.* **71**, 220- 227.

72. Bao, F., Liu, D. (2002) Peroxynitrite generated in the rat spinal cord induces neuron death and neurological deficits. *Neuroscience.* **115**, 839-849.

73. Kalyvas, A., David, S. (2004) Cytosolic phospholipase A2 plays a key role in the pathogenesis of multiple sclerosis-like disease. *Neuron.* **41,** 323-335.

74. Jeffery, N.D., Blakemore, W.F. (1997) Locomotor deficits induced by experimental spinal cord demyelination are abolished by spontaneous remyelination. *Brain* **120,** 27-37.

75. Jasmin, L., Janni, G., Moallem, T.M., Lappi, D.A., Ohara, P.T. (2000) Schwann cells are removed from the spinal cord after effecting recovery from paraplegia. *J Neurosci* **20,** 9215-9223.

76. Kashiwaguchi, S., Masaki, K., Ikata, T. (1989) Experimental studies on permeability of tracers into the spinal cord. *Paraplegia.* **27,** 372-381.

77. Schwartz, E.D., Yezierski, R.P., Pattany, P.M., Quencer, R.M., Weaver, R.G. (1999) Diffusion-weighted MR imaging in a rat model of syringomyelia after excitotoxic spinal cord injury. *Am J Neuroradiol.* **20,**1422-1428.

78. Basso DM, Beattie MS, Bresnahan JC. (1995) A sensitive and reliable locomotor rating scale for open field testing in rats. J Neurotrauma.12(1),1-21.

79. Tosolini, A.P., Morris, R. (2012) Spatial Characterization of the motor neurons columns supplying the rat forelimb. Neurosci. 200, 19-30

80. Lujan, H.L., Palani, G., Peduzzi, J.D., DiCarlo, S.E. (2010) Targeted ablation of mesenteric projecting sympathetic neurons reduces the hemodynamic response to pain in conscious, spinal cord-transected rats. Am J Physiol Regul Integr Comp Physiol. 298(5):R, 1358-65

81. Lujan, H.L., Palani, G., Chen, Y., Peduzzi, J.D., DiCarlo, S.E. (2009) Targeted Ablation of Cardiac Sympathetic Neurons Reduces Resting, Reflex and Exercise-Induced

Sympathetic Activation in Conscious Rats. *Am J Physiol Heart Circ Physiol.* **296**, H1305-H1311,

82. Llewellyn-Smith, I.J., Martin, C.L., Arnolda, L.F., Minson, J.B. (2000) Tracer-toxins: cholera toxin B-saporin as a model. *J Neurosci Methods.* **103(1)**, 83-90.

83. Fargo, K.N., Foster, A.M., Sengelaub, D.R. (2009) Neuroprotective effect of testosterone treatment on motoneuron recruitment following the death of nearby motoneurons. *Dev Neurobiol*. **69(12),** 825-35.

84. Fargo, K.N., Sengelaub, D.R. (2004) Exogenous testosterone prevents motor neuron atrophy induced by contralateral motor neuron depletion. *J Neurobiol.* **60,** 348-359.

85. Gulino, R., Perciavalle, V., Gulisano, M. (2010) Expression of cell fate determinants and plastic changes after neurotoxic lesion of adult mice spinal cord by cholera toxin-B saporin. *Eur. J Neurosci*. **31**:1423-1434

86. Thomson, J., Itskovitz-Eldor, J., Shapiro, S., Waknitz, M., Swiergiel, J., Marshall, V., Jones, J. (1998) Embryonic stem cell lines derived from human blastocysts. *Science.* **282 (5391),** 1145–7.

87. Shamblott, Michael, J., Joyce, A., Shunping, W., Elizabeth, M., Bugg, John, W. L., Peter, J., Donovan, P.D., Blumenthal, G.R., Huggins, John, D.G, (1998) Derivation of Pluripotent Stem Cells from Cultured Human Primordial Germ Cells. *Proceedings of the National Academy of Sciences USA.* **95,** 13726–31

88. Swijnenburg, R.J., Schrepfer, S., Govaert, J.A., Cao, F., Ransohoff, K., Sheikh, A.Y., Haddad, M., Connolly, A.J., Davis, M.M., Robbins, R.C., Wu, J.C. (2008) Immunosuppressive therapy mitigates immunological rejection of human embryonic stem cell xenografts. *Proc Natl Acad Sci U S A*. **105(35)**, 12991-6.

89. Toriumi, H., Yoshikawa, M., Matsuda, R., Nishimura, F., Yamada, S., Hirabayashi, H., Nakase, H., Nonaka, J., Ouji, Y., Ishizaka, S., Sakaki, T. (2009) Treatment of

Parkinson's disease model mice with allogeneic embryonic stem cells: necessity of immunosuppressive treatment for sustained improvement. *Neurol Res.* **31(3),** 220-7.

90. Carlos, L., Pedro, E., José P.V., Catarina, B., Carlo, A. A., Giovanna L., Carlos A., Santana M., Clara, C., Armando, H.F., Jean D. P. (2009) Olfactory Mucosal Autografts and Rehabilitation for Chronic Traumatic Spinal Cord Injury. *Neurorehabil Neural Repair.* **XX(X)**, 1–13.

91. Knoepfler, P.S. (2009) Deconstructing stem cell tumorigenicity: a roadmap to safe regenerative medicine. *Stem Cells.* **27(5)**, 1050-6.

92. Aoi, T., Yae, K., Nakagawa, M., Ichisaka, T., Okita, K., Takahashi, K., Chiba, T., Yamanaka, S. (2008) Generation of pluripotent stem cells from adult mouse liver and stomach cells. *Science*. Aug **1;321(5889)**, 699-702.

93. Boddington, S., Henning, T. D., Sutton, E. J., Daldrup-Link, H. E. (2008) Labeling Stem Cells with Fluorescent Dyes for non-invasive Detection with Optical Imaging. *J. Vis. Exp.* **(14)**, e686

94. Gratzner, H.G., Leif, R.C., Ingram, D.J., Castro, A. (1975) The use of antibody specific for bromodeoxyuridine for the immunofluorescent determination of DNA replication in single cells and chromosomes. *Exp Cell Res.* **95(1)**,88-94.

95. Gratzner, H.G. (1982) Monoclonal antibody to 5-bromo- and 5-iododeoxyuridine: A new reagent for detection of DNA replication. *Science.* **218(4571):**474-5.

96. Parish, C.R. (1999) Fluorescent dyes for lymphocyte migration and proliferation studies. *Immunology and Cell Biology.* **77(6)**: 499–508.

97. Weston, S.A., Parish, C.R. (1990) New fluorescent dyes for lymphocyte migration studies. Analysis by flow cytometry and fluorescence microscopy. *Journal of Immunological Methods.* **133(1),** 87–97.

98. Lyons, A.B., Parish, C.R. (May 1994) Determination of lymphocyte division by flow cytometry. *Journal of Immunological Methods.* **171(1):** 131–7. PMID 8176234

99. Christopher, R. P. (1999) Fluorescent dyes for lymphocyte migration and proliferation studies. *Immunology and Cell Biology.* **77**, 499–508

100. Lippincott-Schwartz, J., Smith, C. L. (1997) Curr. Opin. *Neurobiol.* **7**, 631-639.

101. Stahl, A., Wu, X., Wenger, A. Klagsbrun, M. Kurschat, P. (2005) Endothelial progenitor cell sprouting in spheroid cultures is resistant to inhibition by osteoblasts: A model for bone replacement grafts. *FEBS Lett*. **579**, 5338-5342.

102. Daly, C. J, McGrath, J. C. (2003) Fluorescent ligands, antibodies, and proteins for the study of receptors. *Pharmacol. Ther*. **100**, 101-118.

103. Gao, X. Nie, S. (2005) Methods *Mol. Biol.* **303**, 61-71.

104. Jaiswal, J. K., Goldman, E. R., Mattoussi, H., Simon, S. M. (2004) *Nat. Methods* **1**, 73-78.

105. Bruchez, M. P. (2005) Curr. Opin. *Chem. Biol*. **9**, 533-537.

106. Chan, W. C. (2006) Bionanotechnology progress and advances. Biology of Blood and Bone Marrow Transplantation. *Journal of the American Society for Blood and Bone Marrow Transplantation*. **12**, 87-91.

107. Frangioni, J. V. (2003) In vivo near-infrared fluorescence imaging. *Curr. Opin. Chem. Biol*. **7**, 626-634.

108. Frangioni, J. V. (2006) Self-illuminating quantum dots light the way. *Nat. Biotechnol*. **24**, 326-328.

109. Medintz, I. L., Clapp, A. R., Brunel, F. M., Tiefenbrunn, T., Uyeda, H. T., Chang, E. L., Deschamps, J. R., Dawson, P. E., Mattoussi, H. (2006) Proteolytic activity monitored by fluorescence resonance energy transfer through quantum-dot-peptide conjugates. *Nat. Mater.* **5**, 581-589.

110. Alivisatos, P. (2004) The use of nanocrystals in biological detection. *Nat. Biotechnol*. **22**, 47-52.

111. Marks, K. M., Nolan, G. P. (2006) Chemical labeling strategies for cell biology. *Nature Methods.* **3**, 591-596.

112. Gao, X. Cui, Y. Levenson, R. M. Chung, L. W. Nie, S. (2004) *Nat. Biotechnol*. **22**, 969-976.

113. Stacey, M., Cromer, B., Piotr, W., Jeff, W.M., Bulte. (2011) Tracking stem cells using magnetic nanoparticles. Wiley Interdiscip Rev Nanomed Nanobiotechnol. **3(4),** 343–355.

114. Benoit, D.S., Tripodi, M.C., Blanchette, J.O., Langer, S.J., Leinwand, L.A., Anseth, K.S. (2007) Integrin-linked kinase production prevents anoikis in human mesenchymal stem cells. *J Biomed Mater Res.* **81(2),** 259-68.

115. Nuttelman, C.R., Tripodi, M.C., & Anseth, K.S. (2005) Synthetic hydrogel niches that promote hMSC viability. *Matrix Biol*. **24 (3)**, 208-18

116. Hauger, O., Frost, E.E., van Heeswijk R., Deminiere, C., Xue, R., Delmas, Y., Combe, C., Moonen, C.T.W., Grenier, N., Bulte, J.W.M. (2006) MR evaluation of the glomerular homing of magnetically labeled mesenchymal stem cells in a rat model of nephropathy. *Radiology* **238**, 200–210.

117. Kraitchman, D.L., Tatsumi, M., Gilson, W.D., Ishimori, T., Kedziorek, D., Walczak, P., Segars, W.P., Chen, H.H., Fritzges, D., Izbudak, I., Young, R.G., Marcelino, M., Pittengert, M.F., Solaiyappan, M., Boston, R.C., Tsui, B.M.W. (2005) Dynamic imaging of allogeneic mesenchymal stem cells trafficking to myocardial infarction. *Circulation* **112**:1451–1461.

118. Danielyan, L., Schäfer, R., von Ameln-Mayerhofer A., Bernhard, F., Verleysdonk, S., Buadze, M., Lourhmati, A., Klopfer, T., Schaumann, F., Schmid, B., Koehle, C.,

Proksch, B., Weissert, R., Reichardt, H.M., van den Brandt, J., Buniatian, G.H., Schwab, M., Gleiter, C.H., Frey, W.H. 2nd. (2011) Therapeutic efficacy of intranasally delivered mesenchymal stem cells in a rat model of Parkinson disease. *Rejuvenation Res.* **14(1)**, 3-16.

119. Walczak, P., Zhang, J., Gilad, A.A., Kedziorek, D.A., Ruiz-Cabello, J., Young, R.G., Pittenger, M.F., van Zijl, P.C., Huang, J., Bulte, J.W. (2008) Dual-modality monitoring of targeted intraarterial delivery of mesenchymal stem cells after transient ischemia. *Stroke* **39,** 1569–74.

120. Enyi, S., Teruhisa, K., Xiaojing, J., Naoki, W., Katsushi, Y., Hitoshi, T., Abul Hasan Muhammad Bashar (2006) Intrathecal Injection of Bone Marrow Stromal Cells Attenuates Neurologic Injury After Spinal Cord Ischemia. *Ann Thorac Surg.* **81**, 2227-2234

121. Habisch, H. J., Janowski, M., Binder, D., Kuzma-Kozakiewicz, M, Widmann A, Habich, A., Schwalensto¨cker, B., Hermann, A., Brenner, R., Lukomska, B., Domanska-Janik, K., Ludolph, A.C., Storch, A. (2007) Intrathecal application of neuroectodermally converted stem cells into a mouse model of ALS: limited intraparenchymal migration and survival narrows therapeutic effects . *J Neural Transm.* **114**, 1395–1406

122. Danielyan, L., Schäfer, R., von Ameln-Mayerhofer, A., Buadze, M., Geisler, J., Klopfer, T., Burkhardt, U., Proksch, B., Verleysdonk, S., Ayturan, M., Buniatian, G.H., Gleiter, C.H., Frey, W.H. 2nd. (2009 June) Intranasal delivery of cells to the brain. *Eur J Cell Biol.* **88(6)**, 315-24

123. Pandit, S.R., Sullivan, J.M., Viktoria, E., Alexander, A., Borecki, Sharon, O. (2011) Functional Effects of Adult Human Olfactory Stem Cells on Early-Onset Sensorineural Hearing Loss. *Stem Cells*. **29**, 670–677

124. Nivet, E., Vignes, M., Girard, S.D, Pierrisnard, C., Baril, N., Devèze, A., Magnan, JS, Lanté, F., Khrestchatisky, M., Féron, F., Roman, F.S (2011) Engraftment of human

nasal olfactory stem cells restores neuroplasticity in mice with hippocampal lesions. *Journal of Clinical Investigation.* **121(7)**, 2808–2820

125. Lima, C., Escada, P., Pratas-Vital, J., Branco, C., Arcangeli, C.A., Lazzeri, G., Maia, C.A., Capucho, C., Hasse-Ferreira, A., Peduzzi, J.D. (2010) Olfactory mucosal autografts and rehabilitation for chronic traumatic spinal cord injury. *Neurorehabil Neural Repair.* **24(1)**, 10-22.

126. Rosenkranz, K., Kumbruch, S., Lebermann, K., Marschner, K., Jensen, A., Dermietzel, R., Meier, C. (2010) The chemokine SDF-1/CXCL12 contributes to the 'homing' of umbilical cord blood cells to a hypoxic-ischemic lesion in the rat brain. *J Neurosci Res.* **88(6)**, 1223-33

127. Bittner, G.D., Ballinger, M.L., Raymond, M.A. (1986) Reconnection of severed nerve axons with polyethylene glycol. *Brain Res.* **367,** 351–355.

128. Ramo´n y Cajal S. (1928). Degeneration and regeneration of the nervous system. *Oxford: Oxford University Press.* 1913–1914.

129. Bozkurt, A., Deumens, R., Scheffel, J., O'Dey, D.M., Weis, J., Joosten, E.A., Fu¨hrmann, T., Brook, G.A., Pallua, N. (2008) Catwalk gait analysis in assessment of functional recovery after sciatic injury. *J Neurosci Methods.* **173,** 91–98

130. Campbell, W.W. (2008) Evaluation and management of peripheral nerve injury. *Clin Neurophysiol.* **119**, 1951–1965.

131. Lago, N., Rodriguez, F.J., Guzman, M.S., Jaramillo, J., Navarro, X. (2007) Effects of motor and sensory nerve transplants on amount and specificity of sciatic nerve regeneration. *J Neurosc Res.* **85,** 2800–2812.

132. Radogna, F., Nuccitelli, S., Mengoni, F., Ghibelli, L. (2009) Neuroprotection by melatonin on astrocytoma cell death. *Ann N Y Acad Sci.* **1171,** 509–513.

133. Cai, C., Weisleder, N., Ko, J.K., Komazaki, S., Sunada, Y., Nishi, M., Takeshima, H., Ma, J. (2009) Membrane repair defects in muscular dystrophy are linked to altered interaction between MG53, caveolin-3 and dysferlin. *J Biol Chem.* **284,** 15894–15902.

134. Spaeth, C.S., Fan, J.D., Spaeth, E.B., Robison, T., Wilcott, R., Bittner, G.D. (2011a). Neurite transection produces cytosolic oxidation which enhances plasmalemmal repair. *J Neurosci Res*. (in press).

135. Bittner, G.D., Schallert, T., Peduzzi, J.D. (2000) Degeneration, trophic interactions and repair of severed axons: a reconsideration of some common assumptions. *Neuroscientist.* **6,** 88–109.

136. Deriemer, S.A., Elliott, E.J., Macagno, E.R., Muller, K.J. (1983) Morphological evidence that regenerating axons can fuse with severed axon segments. *Brain Res.* **272,** 157–161.

137. Hoy, R.R., Bittner, G.D., Kennedy, D. (1967) Regeneration in crustacean motor neurons: evidence for axonal fusion. *Science* **156**, 251–252.

138. Neumann, B., Nguyen, K.C.Q., Hall, D.H., Ben-Yakar, A., Hilliard, M.A. (2011) Axonal regeneration proceeds through specific axonal fusion in transected C. elegans neurons. *Dev Dyn.* **240,** 1365–1372.

139. Spaeth, C.S., Robison, T, Fan, J.D., Bittner, G.D. (2012) Cellular Mechanisms of plasmalemmal sealing and axonal repair by polyethylene glycol and methylene blue. *Journal of Neuroscience Research.* **90,** 955-966

140. Krause, T.L., Fishman, H.M., Ballinger, M.L., Bittner, G.D (1994) Extent and mechanism of sealing in transected giant axons of squid and earthworms. *J Neurosci.* **14,** 6638–6651.

141. Bittner, G.D., Keating, C.P., (2012). Rapid, and long lasting behavioral recovery produced by microsutures, methylene blue, and polyethylene glycol after completely cutting rat sciatic nerves. *J.Neurosci.Res.* **90 (5),** 967-80.

ABSTRACT

OPTIMIZATION OF LABELING TECHNIQUES; DETERMINATION OF BEST PARAMETER FOR OMPC DELIVERY AND STUDY OF EFFECTS OF METHYLENE BLUE AND POLYETHYLENE GLYCOL IN AN ANIMAL MODEL OF SPINAL CORD INJURY.

by

Kiran Kumar Rokkappanavar

December 2013

Advisor: Dr. Jean Peduzzi Nelson

Major: Biochemistry and Molecular Biology

Degree: Master of Science

In the United States, the incidence of TSCI is about 40 per million persons per year, with approximately 250,000 living survivors of TSCI in the United States in July 2005. A number of human clinical trials (85) are ongoing using stem cells to evaluate the methods to reduce the injury following TBI. Among the stem cells, olfactory mucosal progenitor cells have several advantages with respect to ease of obtaining, fate of cells, etc. Our study was intended to optimize the labeling technique and to determine the best parameter to deliver the stem cells to the site of injury. We found that CFDA when used at 5 µM concentration, gives good results. We could successfully design an animal model for chemicals induced spinal cord injury using CTB-SAP. Immunofluorescence studies have shown that OMPCs have migrated to the area of injury from the area of injection.

We also aimed to study the effects of polyethylene glycol and methylene blue on the functional recovery following neuronal injury. Results were encouraging as there was significant

functional improvement in BBB scores as a result of using a series of solutions that contain PEG and MB.

AUTOBIOGHRAPHICAL STATEMENT

Father's name: Basavaraj Rokkappanavar

Mother's name: Geetha Rokkappanavar

Date of Birth: July 5, 1984

Country of Origin: India

Education: Bachelor in Medicine and Bachelor in Surgery